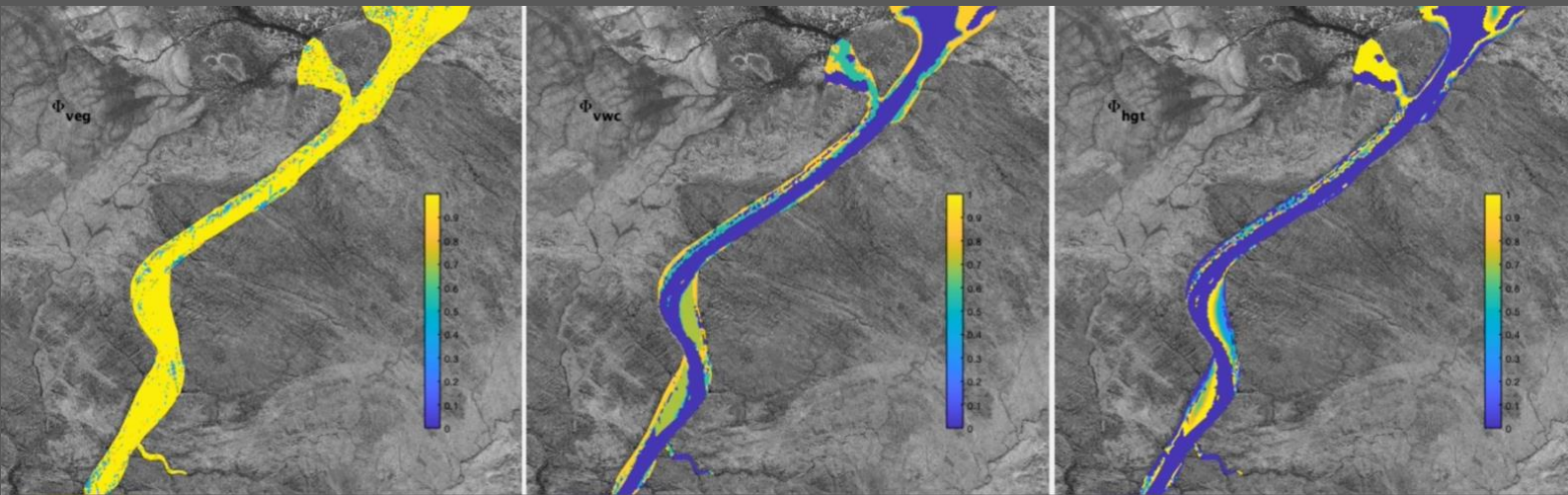




Northern Australia
Environmental
Resources
Hub

National Environmental Science Programme



An eco-hydrological model for assessing riparian habitat: Application to *Passiflora foetida*–crocodile nest interactions at Danggu (Geikie Gorge) National Park

Report

Matthew R. Hipsey, Sherry Zhai, Brendan Busch,
Peisheng Huang, Janaine Zanella Coletti, Ruchira Somaweera,
Bruce L. Webber and Samantha A. Setterfield

© The University of Western Australia, 2021



*An eco-hydrological model for assessing riparian habitat: Application to *Passiflora foetida*-crocodile nest interactions in Geike Gorge* is licensed by The University of Western Australia for use under a Creative Commons Attribution 4.0 Australia licence. For licence conditions see: creativecommons.org/licenses/by/4.0

This report should be cited as:

Hipsey M.R., Zhai S., Busch B., Huang P., Coletti J-Z., Somaweera R., Webber B.L., Setterfield S.A. (2021). An eco-hydrological model for assessing riparian habitat: application to *Passiflora foetida*-crocodile nest interactions at Danggu (Geike Gorge). The University of Western Australia, Perth. Australia.

Cover photographs:

Front cover: Example of output from the eco-hydrological model applied to Danggu for crocodile habitat prediction.

Back cover: Satellite image of the Fitzroy River centred around Danggu (Geike Gorge) National Park.

This report is available for download from the NESP Northern Australia Environmental Resources Hub website at nespnorthern.edu.au

The Hub is supported through funding from the Australian Government's National Environmental Science Program (NESP). The NESP NAER Hub is hosted by Charles Darwin University.

ISBN 978-1-922684-43-1

September, 2021

Printed by UniPrint

Contents

Acronyms & abbreviations	v
Acknowledgements	vi
1. Introduction.....	1
1.1 The need for habitat models	1
1.2 The <i>Passiflora</i> –crocodile case study	1
1.3 Scope of the study	2
2. Model approach	3
2.1 Linking environmental conditions and habitat requirements	3
2.2 River hydrodynamic model	5
2.3 Riparian zone ecohydrology	6
2.3.1 Soil moisture and temperature.....	6
2.3.2 Vegetation water use and interception	6
2.3.3 Vegetation density and shading	8
2.3.4 Feedbacks to river hydrodynamics	8
2.4 Habitat suitability	9
2.4.1 Habitat Suitability Index approach	9
2.4.2 Environmental controls	10
2.4.3 Computing habitat area.....	11
2.5 Model availability and code access	11
3. Danggu (Geike Gorge) application and data requirements	22
3.1 River and floodplain morphometry and mesh generation	22
3.2 Land surface cover and vegetation biomass.....	26
3.3 Hydrological conditions	28
3.4 Meteorological conditions	28
4. Model results	30
4.1 River hydrology	30
4.2 Soil dynamics	30
4.3 Habitat suitability: <i>Passiflora foetida</i>	34
4.4 Habitat suitability: Crocodile nesting.....	38
4.5 Habitat suitability: Interactions	43
5. Conclusions and recommendations.....	49
References	51

List of figures

Figure 1. The habitat index for SP (<i>P. foetida</i>) is calculated in each cell.....	3
Figure 2. Different models form a framework responsible for calculating different variables...	4
Figure 3. A conceptual cell unit of the framework showing the variables calculated by AED-land.....	8
Figure 4. A conceptual cell unit of the framework showing the variables calculated by AED-vegetation.....	9
Figure 5. The integrated model approach is supported by a range of data sourced from different providers.....	22
Figure 6. LiDAR data sub-sampled to 1 m resolution.....	23
Figure 7. Sonar data track within the river channel.	24
Figure 8. Example model mesh, generated after splicing of the sonar and LiDAR data.	24
Figure 9. Final model domain created for the TUFLOW-FV – AED simulation, showing cell bottom elevations.	25
Figure 10. Identification of 5 land cover types based on a guided classification process undertaken on high- quality (cloud-free) dry-season images taken from Sentinel-2.	26
Figure 11. Sub-region plot of (a) the model mesh and cells material classification, and (b) relative cover of vegetation (area fraction).	27
Figure 12. Local weather data collected within the Geike Gorge domain in 2017, within and outside of a nest location.	28
Figure 13. Local data collected within the Geike Gorge domain in 2017, within and outside of a nest.	29
Figure 14. Example output from the hydrodynamic model, compared with observed flow data (bottom right inset).	30
Figure 15. Example output from the ecohydrology model for a chosen cell, showing the long-term meteorological drivers of soil temperature and soil moisture (VWC).....	32
Figure 16. Example output from the ecohydrology model showing the spatial predictions of the model substrate (MATZ), temperature (water or soil surface), soil moisture (VWC), bathymetry (BATHY), and the wettime (WET) and drytime (DRY) outputs.	33
Figure 17. Output from the habitat model for 2016 conditions showing variability in environmental factors contributing to SP adult plant growth, based on average conditions throughout the relevant period (March to July).	35
Figure 18. Output from the habitat model for 2016 conditions showing variability in environmental factors contributing to SP seedling establishment, based on average conditions throughout the relevant period (January to March).....	36
Figure 19. Output from the habitat model for 2016 conditions showing variability in environmental factors contributing to SP resprouting likelihood, based on conditions throughout the relevant averaging period (January to March).	37
Figure 20. Comparison of composite HSI values for Passiflora (mean of SP HSI for the plant, sprout and seed life- stages) and the Sentinel-estimated Passiflora coverage data.....	38

Figure 21. Output from the habitat model for 2016 conditions showing variability in environmental factors contributing to AFC nesting habitat, based on average conditions throughout the relevant period (March to July).	40
Figure 22. Output from the habitat model for 2016 conditions showing variability in environmental factors contributing to SP seedling establishment, based on average conditions throughout the relevant period (January to March).	41
Figure 23. Output from the habitat model for 2016 conditions showing variability in environmental factors contributing to SP resprouting likelihood, based on average conditions throughout the relevant period (January to March).	42
Figure 24. Monitoring data from Somaweera et al. (2021), left, showing identified nests and hatchling occurrence in the 2016 dry season, compared with the model predictions of the 2016 nesting HSI, right.....	43
Figure 25. Summary of the habitat model output showing average HSI for different life-stages of SP and AFC within the relevant periods.	44
Figure 26. Monitoring data from Somaweera et al. (2021) showing identified nests and hatchling occurrence between 2016 and 2019.	45
Figure 27. Summary of the habitat model output for AFC life-stages (top) and difference (Δ) if the effect of <i>Passiflora</i> is removed.....	46
Figure 28. Effective area of suitable habitat (A^{HSI}/AT) for different life stages of SP and AFC.....	47
Figure 29. Nests (red dots) located within a <i>P. foetida</i> patch at Danggu.....	48

List of tables

Table 1. List of models and modules that comprise the modelling framework.	5
Table 2. Life-stage time windows over which environmental suitability is assessed.....	10
Table 3. Habitat requirements that define the habitat index for stinking passionflower (SP), P. foetida.....	12
Table 4. Habitat requirements that define the habitat index for the Australian freshwater crocodile (AFC), <i>Crocodylus johnstoni</i>	19

Acronyms & abbreviations

2D, 3D	two-dimensional, three-dimensional
AED	Aquatic EcoDynamics water quality and aquatic habitat model platform
AFC	Australian freshwater crocodile
BOM	Bureau of Meteorology
DBCA	Department of Biodiversity, Conservation and Attractions (WA)
DEM	Digital elevation model
DWER	Department of Water and Environmental Regulation (WA)
HSI	Habitat Suitability Index
LAI	Leaf Area Index
LiDAR	Light Detection and Ranging
mAHD	metres above the Australian Height Datum
NAERH	Northern Australia Environmental Resources Hub
NESP	National Environmental Science Program
pers. comm.	personal communication
SDM	Species distribution models
SP	Stinking passionflower
TUFLOW-FV	Finite Volume Hydrodynamic Model released by BMT Global Pty Ltd

Acknowledgements

We gratefully acknowledge the assistance by Hasnein bin Tareque for undertaking the Sentinel satellite imagery classification. We also thank BMT Pty Ltd for providing the TUFLOW-FV model for application on this project and supporting custom modifications to support the habitat prediction requirements.

We acknowledge the Western Australian Department of Biodiversity, Conservation and Attractions, CSIRO, and the Australian Government's National Environmental Science Program for funding this work.

1. Introduction

1.1 The need for habitat models

The conservation of biota depends on optimisation of the quality *and* quantity of their habitat (Jacobsen and Kleynhans, 1993). However, specifically defining the habitat requirements of species can be challenging due to the range of potential interacting factors that must be identified and characterised through time and space. Whilst some factors can be defined in specific terms (e.g., temperature requirement), other factors may only be able to be identified in qualitative terms, based on *ad hoc* or anecdotal observations, making it difficult to be able to define habitat quality in a quantitative manner. However, when management interventions are being designed to assist in the conservation or restoration of an environmental system, having methods able to support a quantitative comparison of habitat is essential to be able to support decision-making. New methods are needed to help managers assess what is good habitat for essential species, and how proposed management measures may increase or decrease habitat quality and extent (Walters and Korman, 1999). Bearing in mind data limitations, these methods need to be able to be applied in situations with incomplete or patchy datasets, incorporating expert knowledge and practical for end-users.

Riparian ecosystems in particular support a diversity of habitat that are essential to support the health of river basins, spanning laterally across river reaches, and along the river continuum (Randhir and Ekness, 2013). These systems support diverse ecosystem services and can be hotspots of biodiversity as they exhibit a gradient of conditions spanning from aquatic to terrestrial. The nature of riparian habitat changes based on river flow regimes – under typical cycles of flow variation, pseudo-steady structure in riparian ecosystems can form, but particularly large flood events or long drought periods can cause long-term shifts in riparian conditions. While riparian systems are therefore quite dynamic, active management can prevent them from degradation and loss where risks are identified.

Managing riparian ecosystems in northern Australia to improve the quality and extent of this important habitat is a key focus area of the National Environmental Science Program's (NESP's) Northern Australian Environmental Resources Hub of (NAERH). Loss of riparian habitat can occur due to altered hydrology in rivers and catchments, physical degradation due to development activities, and degradation brought about by non-native invasive species. This project was undertaken in NESP NAERH Project 2.6 with the aim to develop an ecohydrology model approach able to simulate and assess habitat quality and extent and that is suitable to support assessment of future risks from changing water regimes. Specifically, the model approach is prototyped using the Danggu (Geike Gorge) National Park on the Fitzroy River as a case study. Danggu (Geikie Gorge) is included in the West Kimberley National Heritage Place and has significant cultural and intrinsic biodiversity values, and may be impacted in the future by changes to water availability in addition to having numerous challenges associated with non-native invasive species.

1.2 The *Passiflora*–crocodile case study

Non-native invasive plants in Australia represent not only a significant cost to agriculture and directly threaten native biological diversity (Ziska and Dukes, 2014). Stinking passionflower (SP; *Passiflora foetida*) is a threatening weed that has been reported to cause a significant

negative impact on ecosystem values in northern Australia (Jucker et al., 2020), particularly riparian and other freshwater ecosystems. In the Fitzroy River, located in the Kimberley region of Western Australia, preliminary site observations revealed that *P. foetida* has been preventing the Australian freshwater crocodile (AFC; *Crocodylus johnstoni*) from using sand banks by covering and altering the environments typically relied upon for nesting. There is therefore concern that the expansion of the threatening weed may lead to shrinking habitat areas for *C. johnstoni*.

The environmental requirements of freshwater crocodiles have not been determined for any river system in Australia (Pusey and Kath, 2015). To date, it is known that the eggs of the *C. johnstoni* require a certain soil moisture and soil temperature during incubation (Somaweera and Shine 2013). As *P. foetida* can form thick mats over the ground and smother nests, it could therefore alter the habitat available for *C. johnstoni* nesting, not only by covering suitable beaches, but also by affecting local soil moisture and temperature that would impact eggs during incubation.

To successfully manage the spread of *P. foetida* and the potential habitat left for *C. johnstoni* in the Fitzroy River, it is necessary to predict the spread of *P. foetida*, given the possible range of climatic and hydrological conditions forecasted for the region. Physical, biological or chemical methods can typically be used to control the spread of non-native invasive species (Chandrasena and Johnson 2015), though this is logistically difficult in remote river regions where SP takes hold. Extensive flooding also controls *P. foetida* extent, as plant growth is inhibited and seedlings are unlikely to establish when submerged for a period. Planned flooding therefore represents one possible management option in regulated rivers. While this can represent a negative impact in many instances (sediment retention, fish migration interruptions, etc.), understanding how manipulation of river level could potentially impact on *P. foetida* and AFC populations is of interest.

1.3 Scope of the study

The aim of this study has been to develop an ecohydrological model able to provide the essential environmental parameters necessary to assess and quantify habitat of *P. foetida* and *C. johnstoni*. We developed a prototype approach that is a combination of an environmental model and a habitat suitability model suitable for riparian environments. The environmental model can simulate river and floodplain hydrodynamics in addition to soil moisture and temperature in the riparian zone. We then created habitat suitability models of the two species based on a literature review, results from experimental and field research, and expert judgement. This predictive tool is able to provide an estimate of the likelihood of weed occurrence, and the nature of how this will interact with the habitat needed for successful crocodile nesting and hatchling success.

This report outlines the approach to model development, the application and setup of the model to Danggu (Geike Gorge) National Park – part of the Fitzroy River in Western Australia – and presents the results of habitat predictions from simulations undertaken at this site with the new coupled model approach.

2. Model approach

2.1 Linking environmental conditions and habitat requirements

The model approach adopted combines an environmental model and a habitat model tailored to resolve riparian habitat features relevant to SP and AFC preferences. The environmental model is built on a spatially resolved river hydrodynamic model that accounts for local topographic data and resolves spatio-temporal variability in water level, velocity and temperature. The model is adapted to capture the history of a cell's inundation, such that as an area becomes dry, the exposed soil is subject to desiccation and the vertical soil moisture profile will respond to evaporation and rainfall events. The soil and water temperature in both river and riparian zone cells are computed based on a surface energy balance and can resolve the various thermal diffusivities of different substrates, plus the effect of shading by low and high vegetation canopy cover. The approach is therefore part mechanistic (explicitly resolving soil moisture and soil temperature) and part empirical (adopting expert judgment and empirical tolerance data to map the 'habitat index' as a proxy for species success, rather than explicitly resolving the crocodiles egg maturation or plant biomass, for example). The model implementation is depicted in Figure 1.

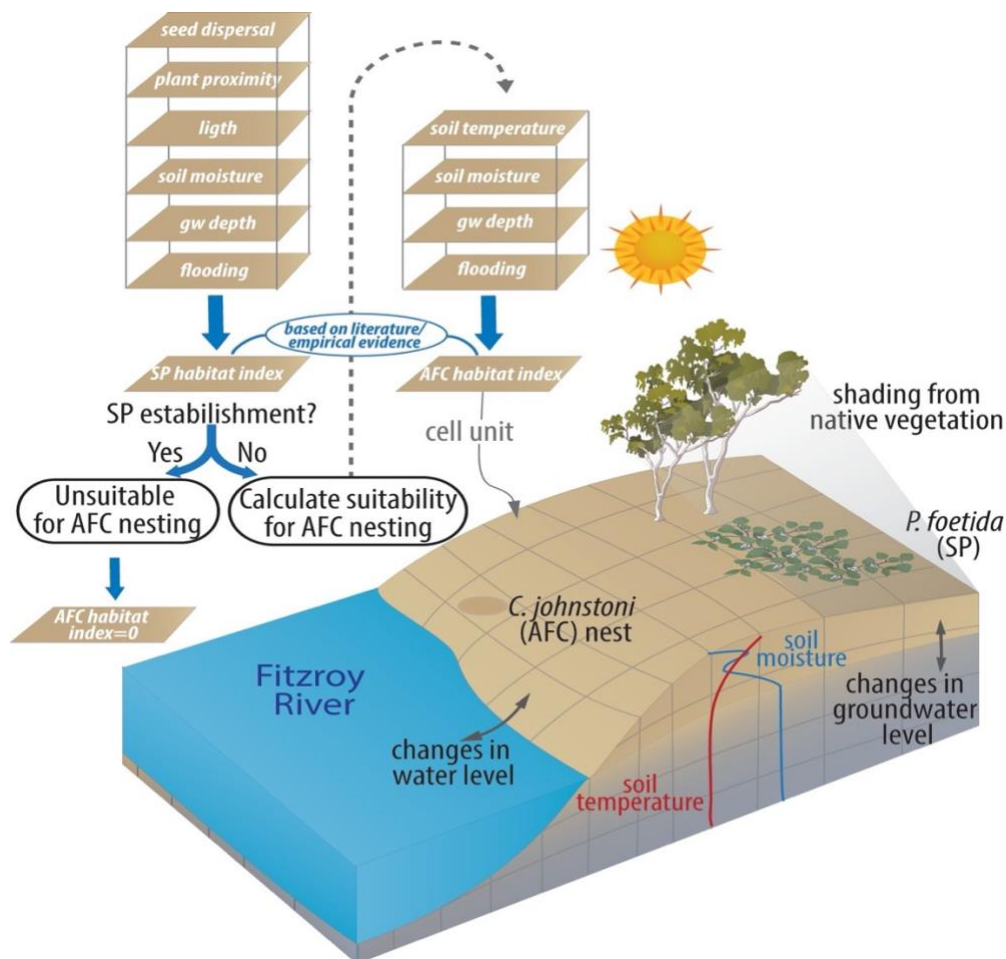


Figure 1. The habitat index for SP (*P. foetida*) is calculated in each cell. If SP is likely to establish in that cell, it is deemed unsuitable for AFC nesting and the habitat index for AFC is zero. Otherwise, the model proceeds to evaluate the habitat index for AFC.

The base platform for capturing the river hydrodynamics is `TUFLOW-FV` (BMT 2019), and the riparian ecohydrology and habitat model is simulated by the `AED` modelling library (Hipsey et al., 2019). The coupled model adopts a flexible mesh numerical domain and each cell can have different soil substrates defined and vegetation presence. Different modules within the framework are then responsible for sequentially calculating the relevant variables in each cell unit depending on its, wet/dry status (Figure 2). Water level is mechanistically resolved by `TUFLOW-FV` whereas soil moisture, soil temperature and groundwater level are resolved by `AED-land`. Shading by native vegetation (important variable to estimate soil temperature) is resolved by `AED-vegetation`. After calculating the environmental variables, `AED-habitat` empirically assesses the Habitat Suitability Index (HSI) for SP and AFC. Table 1 summarises the variables simulated in each model cell. The predicted HSI varies from zero to one for a given cell at each time-step, following integration of the index over a relevant establishment period, a low value indicates conditions are unsuitable for establishment or nesting and a value close to one indicates conditions are suitable. The modules are linked and can interact, such that, if the HSI is rated to be high for SP, the same cell will take this into account when computing AFC. A detailed description for each sub-model is provided in the following sections.

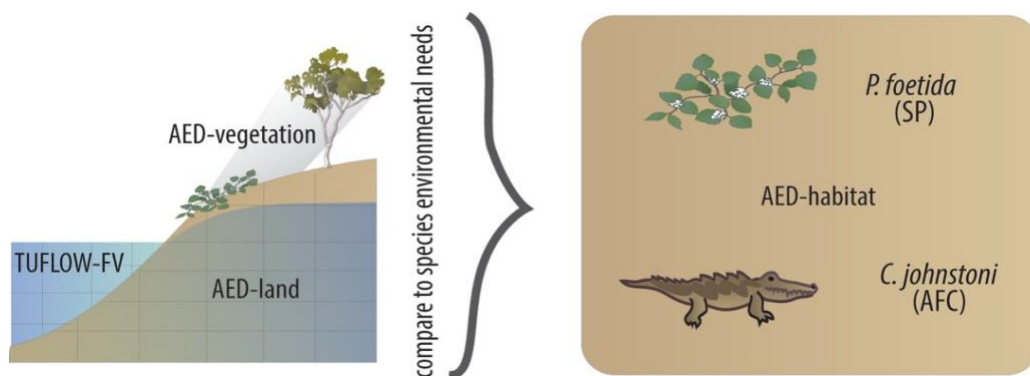


Figure 2. Different models form a framework responsible for calculating different variables. `AED-habitat` then compare those variables to the species needs.

Table 1. List of models and modules that comprise the modelling framework. Variables are described as mechanistically resolved (**mech**), empirically estimated (**emp**), or as a boundary condition (**bc**).

Variable	Model/module	Description
h, z	TUFLOW-FV	water level and depth (<i>mech</i>)
u, v		water velocity (<i>mech</i>)
T		water temperature (<i>mech</i>)
h_{gw}	AED-land	groundwater height (<i>bc</i>)
$\theta(z)$		soil moisture, as a function of depth (<i>mech</i>)
$T(z)$		soil temperature, as a function of depth (<i>mech</i>)
V	AED-vegetation	over-storey vegetation biomass (<i>bc</i>)
P		under-storey vegetation biomass (<i>bc</i>)
LAI		aggregate leaf-area-index (<i>emp</i>)
Φ_{sp}^{HSI}	AED-habitat	Habitat Index – <i>Passiflora</i> establishment (<i>emp</i>)
Φ_{afc}^{HSI}		Habitat Index – Crocodile nesting/hatchling suitability (<i>emp</i>)

2.2 River hydrodynamic model

The river hydrodynamic model used to simulate water movement and riparian zone wetting and drying is the TUFLOW-FV platform (www.tuflow.com). The model uses a 2D/3D flexible-mesh, finite volume approach to solve the shallow water equations. The platform supports a range of customisations for specifying boundary conditions and hydraulic controls allowing users to simulate water level, water velocity and water temperature in response to meteorological and variable hydrological forcing.

The mesh consists of triangular and quadrilateral elements of different size and can be used to capture areas of complex morphometry. Whilst the model supports three-dimensional simulations, for example to resolve vertical density stratification, in this application we adopt a depth-averaged 2D approach for simplicity. Each cell is configured to have a defined substrate and bottom roughness that influence water flow and mixing through a custom drag calculation. Wetting and drying of riparian cells is captured in response to local water level changes and a threshold water-depth condition.

Diurnal and seasonal changes in water temperature are simulated by resolving the surface energy balance, accounting for penetrative and non-penetrative fluxes of heat based on user-provided local meteorological conditions (e.g. solar radiation, cloud cover, humidity and temperature). This accounts for water loss through open-water evaporation, and contributions from rainfall. Application of the model to a range of rivers is presented in Brookes and Hipsey (2019).

2.3 Riparian zone ecohydrology

The Aquatic Ecodynamics (AED) modelling library is an open-source community-driven library of model components for simulation of water quality, aquatic ecosystem dynamics as well as terrestrial and aquatic habitats. The AED library consists of numerous modules that are configured according to ecosystem conceptualisations. This application adopts the more advanced modules for soil dynamics and vegetation, both of which are able to operate in dry and inundated cells of the mesh. Based on the soil and vegetation dynamics, feedbacks to the hydrodynamic water are resolved, accounting for the effects of solar shading, canopy rainfall interception, or groundwater seepage.

2.3.1 Soil moisture and temperature

The soil moisture and temperature model in AED-land is a vertically resolved model typically using 20 layers below the soil surface that solves a heat and water balance based on Richard's Equation. The model implementation is based on the NicheMapR implementation of the Campbell soil physics model outlined in detail in Kearney et al. (2016); depicted conceptually in Figure 3. Water uptake from vegetation is taken from across the soil layers.

2.3.2 Vegetation water use and interception

Vegetation water-use and rainfall interception is undertaken in AED-vegetation. Throughfall, P , is the incoming precipitation after interception losses, defined as:

$$P = P_t - i_{\max} \frac{LAI}{LAI_{\max}} \quad (1)$$

where:

P_t is the above-canopy precipitation rate (m/d)

i_{\max} is the maximum rate of precipitation interception (m/d)

LAI_{\max} is the maximum LAI, determined by the carrying capacity (m^2/m^2).

The potential evapotranspiration, E_0 (m/d), depends on the relative humidity, solar radiation, wind speed and air temperature, according to the Penman-Monteith equation (Allen et al., 1998):

$$E_0 = \left[\frac{0.408 \Delta (R_n - G) + \gamma \left(\frac{t_y}{T + 273} \right) u_2 VPD}{\Delta + \gamma (1 + 0.34 u_2)} * 1000 \right] \quad (2)$$

where:

$$t_y = \begin{cases} 900, & \text{if } dt = 86400 \text{ s} \\ 37, & \text{if } dt = 3600 \text{ s} \end{cases}$$

T = air temperature at 2 m height ($^{\circ}\text{C}$)

VPD = vapour pressure deficit (kPa)

u_2 = wind speed at 2 m high (m/s)

R_n = net radiation at the crop surface ($\text{MJ}/\text{m}^2/\text{d}$)

Δ = slope vapour pressure curve ($\text{kPa}/^{\circ}\text{C}$)

γ = psychrometric constant ($\text{kPa}/^{\circ}\text{C}$)

G = soil heat flux density ($\text{MJ}/\text{m}^2/\text{d}$)

Plant transpiration, E (m/d), is modelled as a function of the plant water uptake rate, W , and E_0 :

$$E = \Psi E_0 \quad (3)$$

where Ψ (-) is the normalized potential water uptake (Skaggs et al., 2006).

The evaporation from bare soil, E_b (m^3/d), is calculated based on the potential evaporation, E_0 . If the soil is not saturated, the ratio of θ to water content at field capacity, θ_{fc} , is also considered as a scaling factor (Aydin et al., 2005). Further, evaporation from bare soil is adjusted based on total LAI (sum of all vegetation types) to reflect the cover that vegetation causes due to shading of the exposed soil surface. Therefore, the evaporative rate respectively, are:

$$E_{bS} = E_0 \left(1 - 0.9 \frac{\text{LAI}_S}{\text{LAI}_{\max}} \right) \quad (4)$$

and

$$E_{bU} = E_0 \left(1 - 0.9 \frac{\text{LAI}_U}{\text{LAI}_{\max}} \right) \left(\frac{\theta}{\theta_{fc}} \right) \quad (5)$$

Note that from a computational point of view, the infiltration rate is calculated based on the soil moisture from the previous day, which means that at the first day the water table level reaches ground level, infiltration can be different from zero. In this case, the excess volume is diverted to the river as surface runoff by adding to Q_{se} .

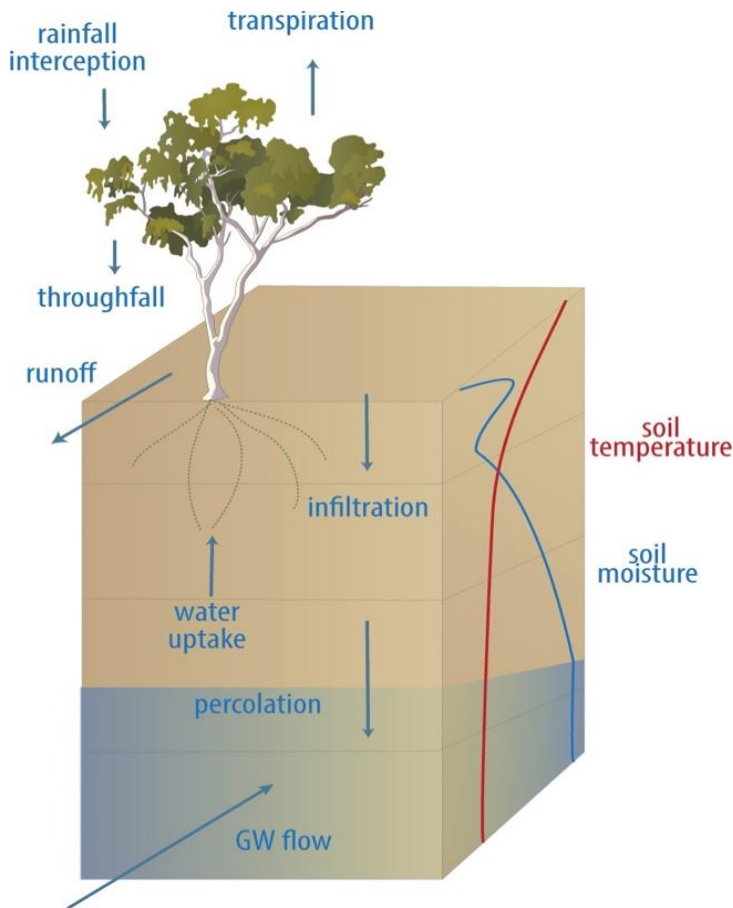


Figure 3. A conceptual cell unit of the framework showing the variables calculated by *AED-land*.

2.3.3 Vegetation density and shading

Vegetation presence and shading of the soil or surface water is also undertaken in *AED-vegetation*. For this application context, the native vegetation is assumed as having a seasonal variation but is not affected by climate and hydrological forcing. A satellite imagery-based estimate of the vegetation was converted into a vegetation density, LAI (leaf area index). LAI then is used to predict the rainfall interception, transpiration and shading.

Vegetation presence in a given cell can contribute to shading (Figure 4) depending on the cell's LAI, according to a linear attenuation function. This reduces the incident light used as the surface boundary condition for the soil heating or water column heating routines.

2.3.4 Feedbacks to river hydrodynamics

In each unit cell of the domain and at each time-step, *AED-land* solves the water balance and communicates its results to *TUFLOW-FV*, which then transports the water within the river

domain. AED-vegetation also updates TUFLOW-FV about the shading of the wet cells. The model also track the time that each cell has been wet or dry (“wetime” and “drytime”).

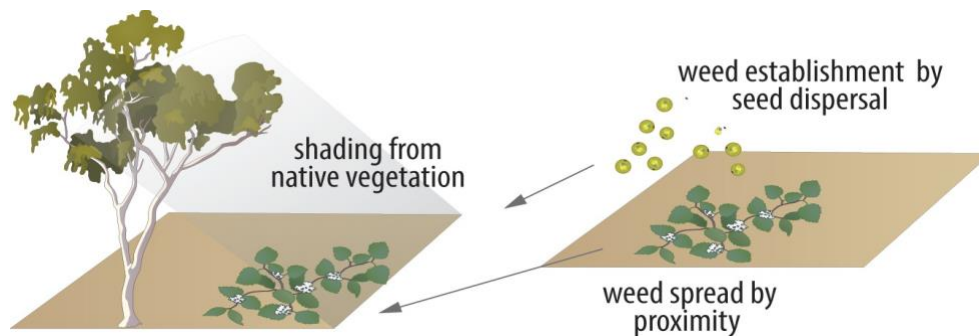


Figure 4. A conceptual cell unit of the framework showing the variables calculated by AED-vegetation.

2.4 Habitat suitability

In contrast to models that simulate the explicit dynamics of plant or crocodile biomass, an alternative approach is to simulate a “habitat index”, based on a multi-criteria assessment of modelled conditions relative to the known environmental requirements of SP and AFC. The AED-habitat module has been customised to include functions that consider historical observations of species occurrence and associated literature on species environmental needs with environmental estimates to calculate a habitat index. As such, AED-habitat compares the soil moisture, soil temperature, light and/or other environmental conditions calculated by other modules within the framework. Similar to species distribution models or SDM (Elith and Leathwick, 2009), this approach empirically defines conditions that lead to successful growth and reproduction, without simulating processes such as photosynthesis or bioenergetics.

After calculating the likelihood of SP to establish in a certain cell, the framework predicts the suitability for AFC nesting, egg incubation and hatchling success (Figure 1). In addition to an area free from SP, the requirements for AFC to nest in a certain cell are defined by the soil moisture and soil temperature and proximity to the water. The framework assumes that, once the requirements to the establishment of SP are met in a certain cell, SP will gradually occupy the cell, deeming it less suitable for AFC nesting while SP continues to occupy the cell. In cells with a low likelihood of SP (either due to unsuitable conditions from early in the season, or becoming less suitable during the simulation, such as due to flooding) the environmental constraints for AFC will be more important in controlling suitability.

2.4.1 Habitat Suitability Index approach

In each model cell (c), the Habitat Suitability Index (HSI) is computed based on suitability of conditions (i), for each of the pre-defined critical life-stages (j), by defining a fractional index, $\Phi_i^{HSI_j}$. The fractional index for each attribute is computed at each time-step and then integrated over a specified time window, specific to the life-cycle stage. Stages are

considered based on expert judgement of critical requirements for SP and AFC to successfully reproduce.

$$\Phi_i^{HSIj} = \frac{1}{t_{jstart}-t_{jend}} \sum_{t=t_{jstart}}^{t_{jend}} \Phi_i^{HSIj}(i)_t \quad (6)$$

whereby: $i = \{\text{environmental conditions}\}$
and: $j = \{\text{life} - \text{stage}\}$

The integration time for each life-stage, j , is set based on expert judgement and assessment of literature on the typical times reported.

Whilst this description is generic for any species, for this application we specifically define three 'life-stages' for each of the two species of interest (Table 2). The environmental conditions for each cell of the model are resolved at high spatio-temporal resolution, but the integration (sum symbol) in Eq. 6 is applied to the species-specific time windows defined for each stage. Therefore the algorithm above is computed in each cell and produces maps of suitability (between 0 and 1) for each environmental attribute for each life-stage within any given year.

Table 2. Life-stage time windows over which environmental suitability is assessed.

	SP			AFC		
Life stage, j	Seedling establishment	Adult resprouting	Adult growth & fruiting	Nesting	Incubation	Hatching
Start date, t_{jstart}	Jan	Jan	Mar	Mid-Aug	Mid-Aug	Nov
End date, t_{jend}	Mar	Feb	Jul	Mid-Sep	Early Nov	Dec

2.4.2 Environmental controls

The individual functions for the environmental responses are generally piecewise, based on synthesis of the available literature. For this study we defined environmental factors of importance as being air and soil temperature, soil moisture, light availability, water velocity and depth, substrate type; these are summarised in detail for SP (Table 3) and AFC (Table 4).

These are then overlaid to produce a final map for any given year for each life-stage using:

$$\Phi_c^{HSI} = \min [\Phi_i^{HSIj}]_c \quad (7)$$

2.4.3 Computing habitat area

To compare the overall area of suitable habitat between years, or the relative suitability of alternate scenarios, the fractional suitability is used as a multiplier with the cell area, according to:

$$A^{HSI} = \sum_c \Phi_c^{HSI} A_c \quad (8)$$

and the spatially averaged HSI in any given region (with area A) is computed as:

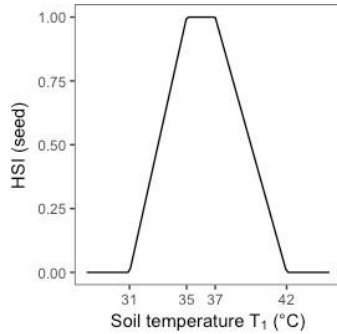
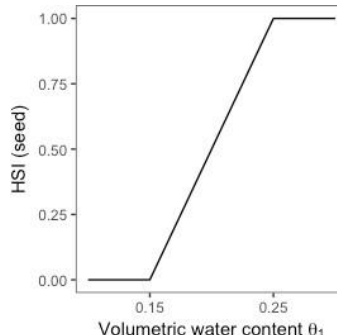
$$\overline{HSI} = \frac{1}{A} \sum_c \Phi_c^{HSI} A_c \quad (9)$$

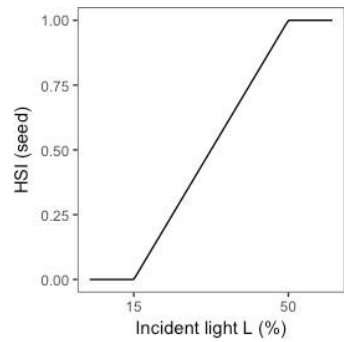
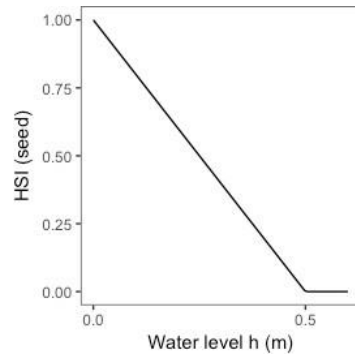
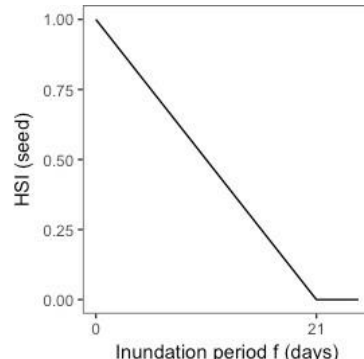
2.5 Model availability and code access

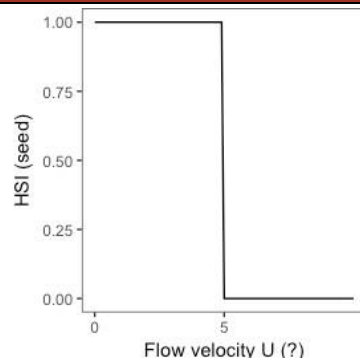
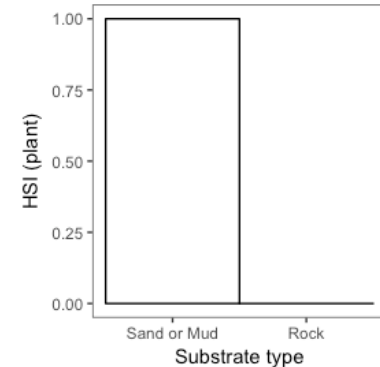
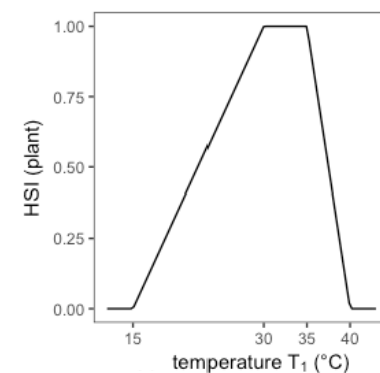
The SP and AFC habitat models, based on the above algorithms and functions in Table 3 and Table 4, are released as open-source as part of the AED model platform in the `libaed-riparian` library. Code can be accessed from <https://github.com/AquaticEcoDynamics/libaed-riparian>

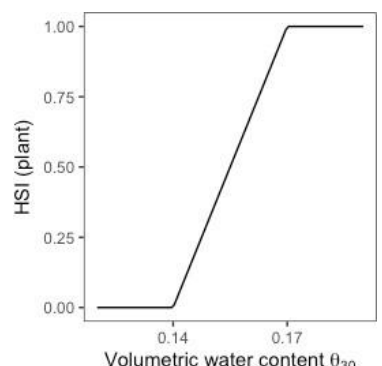
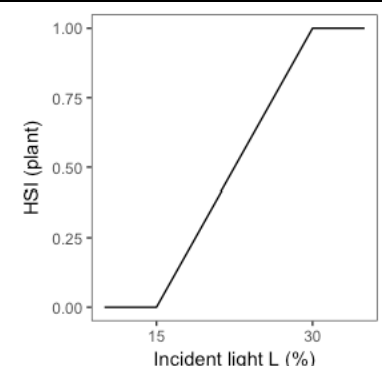
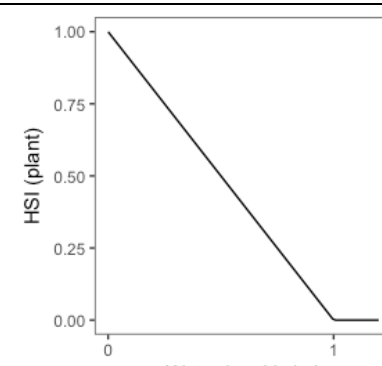
A pre-compiled AED dll plug-in file with the above library is available from the authors on request. Users can access the hydrodynamic platform TUFLOW-FV from <http://www.tuflow.com> – a range of support utilities and access options for use of the model are available. The model may be operated through a QGIS plug-in, though in this report we manually ran the model and used MATLAB for file and figure processing.

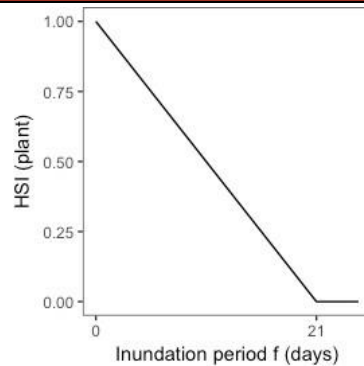
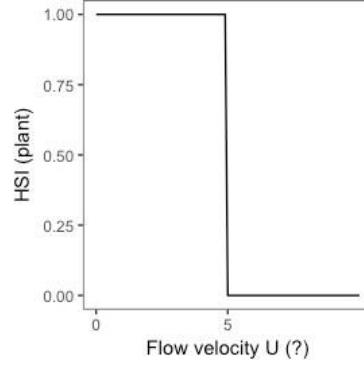
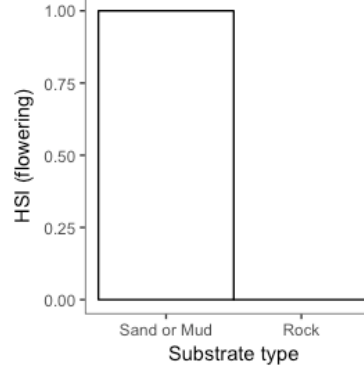
Table 3. Habitat requirements that define the habitat index for stinking passionflower (SP), *P. foetida*.

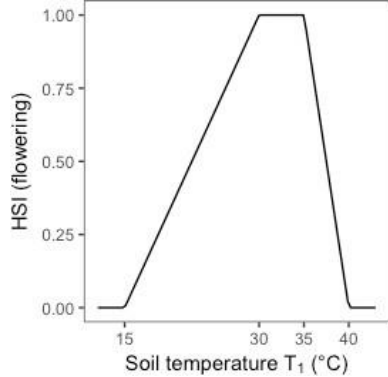
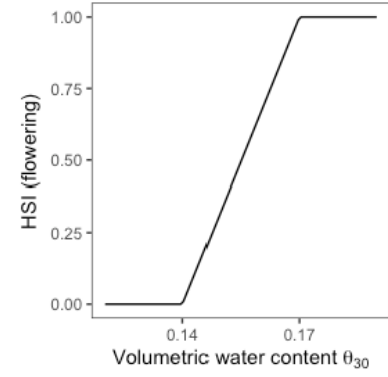
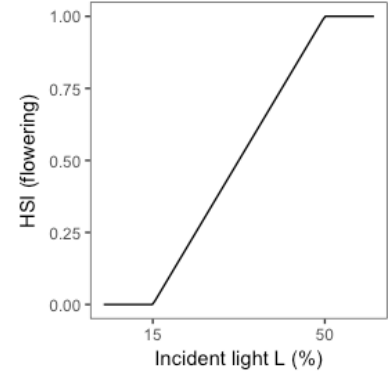
Life stage (j)	Environmental condition (i)		Habitat Suitability Index (Φ)		Rationale	Source	Comment
Seedling establishment (Jan–Mar)	Sub	Substrate type	Φ_{sub}^{seed}		All substrate types are suitable	Webber (pers. comm.)	Silt or loam environments may be more indicative as they are likely to be more depositional/accumulation areas
	T_1	Air temperature (°C)	Φ_{tem}^{seed}		Temperature is a significant determinant of total germination of <i>P. foetida</i> seeds.	White (2017), Findlay (2019)	Experiment used air temp. Seedlings won't establish in hot sand for example
	θ_1	Soil volumetric water content at 1 cm depth	Φ_{vwc}^{seed}			Findlay 2019, Webber et al. (2014)	Findlay (2019) found highest germination (62–81%) with high moisture availability ($\Psi = 0$ MPa). No germination was observed for water potential (Ψ) treatments of -1.05, -1.4 and -1.75 MPa, and minimal germination observed for water potential treatments of -0.7 and -0.35 MPa (< 25% and < 50% respectively).

Life stage (j)	Environmental condition (i)		Habitat Suitability Index (Φ)		Rationale	Source	Comment
	L	Percentage of incident solar irradiance available to plant (%)	Φ_{veg}^{seed}				Little evidence found on the effect of light on germination, hence assumed the same as adult plant.
	h	Water level during inundation (meter)	Φ_{dep}^{seed}		Establishment is less likely under water	Webber (pers. comm.)	
	f	Period of inundation (days)	Φ_f^{seed}		Prolonged inundation inhibit growth and increases the risk of seed/seedling damage	Webber (pers. comm.)	In addition to the effect of inundation itself, some inundation-related effects may be at play: (1) impaired photosynthesis due to high sediment load in the water, (2) aquatic herbivory

Life stage (j)	Environmental condition (i)		Habitat Suitability Index (Φ)		Rationale	Source	Comment
Seedling production (Jan–Mar)	U	Inundation flow velocity (m/s)	Φ_{vel}^{seed}		Moderate velocity will remove seed given their small size	Webber (pers. comm.)	Critical velocity assumed
Adult plant growth (Mar–Jul)	Sub	Substrate type	Φ_{sub}^{plant}		Plants will grow well on sand or mud, and can establish in cracks between rocks with otherwise minimal topsoil/sand.		
	T_{20}	Air temperature (°C)	Φ_{tem}^{plant}		Air temperature significantly affects plant survival and biomass accumulation rate	White (2017)	15°C is a guess as experiment did not reach lower limit. Webber set 15°C as ‘cold stress’ in their model (which is air temp). Experiment used air temp.

Life stage (j)	Environmental condition (i)		Habitat Suitability Index (Φ)		Rationale	Source	Comment
	θ_{20}	Soil volumetric water content at 20 cm depth	Φ_{vwc}^{plant}		Growth is severely constrained at low soil moisture	White (2017)	
	L	Percentage of incident solar irradiance available to plant (%)	Φ_{veg}^{plant}		Irradiance level has a profound effect on plant survival, growth and biomass accumulation	Webber (pers. comm.), Barrs and Kelly (2012) (on another <i>Passiflora</i> sp. 2%<L<=40% (max tested))	Lower limit unknown, assume same as seed (15%), could be lower. Shading will slow biomass accumulation.
	h	Water level during inundation (meter)	Φ_{dep}^{plant}		Plants will reduce growth during inundation	Webber (pers. comm.)	Critical water level assumed

Life stage (j)	Environmental condition (i)		Habitat Suitability Index (Φ)		Rationale	Source	Comment
	f	Period of inundation (days)	Φ_f^{plant}		Studies show seedlings survive > 3 weeks with full inundation. On other <i>Passiflora</i> sp., young plants are very adaptive to flooded conditions (tested up to 7 days 2cm h)	Webber et al. (2018), Govêa et al. 2018	
	U	Inundation flow velocity (m/s)	Φ_{vel}^{plant}		High velocity will physically remove plants (above ground biomass will be removed first before below ground biomass. At fast flow, both above and below ground biomass will be removed)	Webber (Pers. comm.)	Critical velocity assumed
Adult resprouting (Jan–Mar)	Sub	Substrate type	Φ_{sub}^{sprout}			Florabase	This is linked to the previous year's Φ -/01'

Life stage (j)	Environmental condition (i)		Habitat Suitability Index (Φ)		Rationale	Source	Comment
	T_1	Air temperature (°C)	Φ^{sprout}_{tem}				Assumed same as adult plant
	θ_{20}	Soil volumetric water content at 20 cm depth	Φ^{sprout}_{vwc}		Resprouting becomes less likely if plant subjected to drought		
	L	Percentage of incident solar irradiance available to plant (%)	Φ^{sprout}_{veg}				Assumed same as adult plant

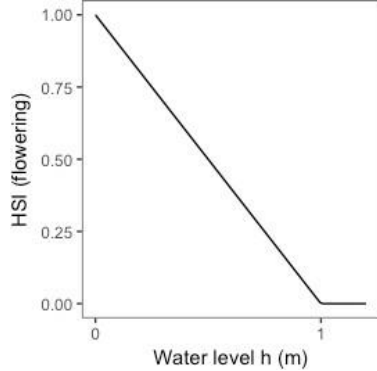
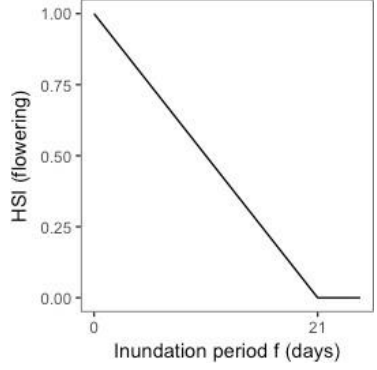
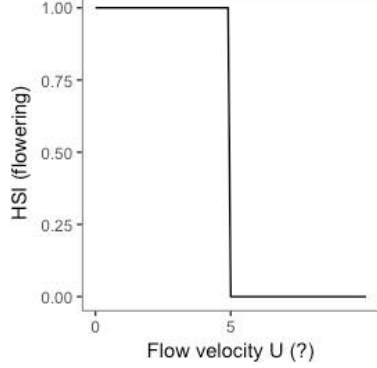
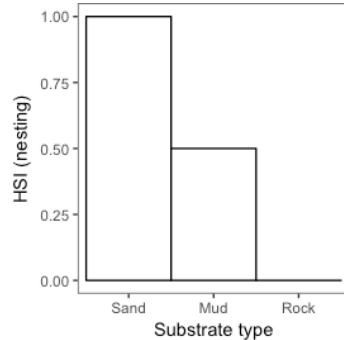
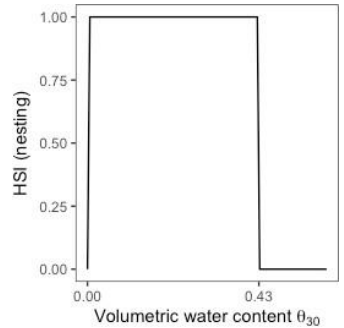
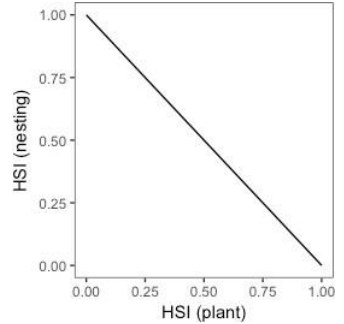
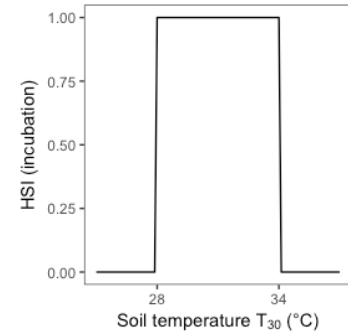
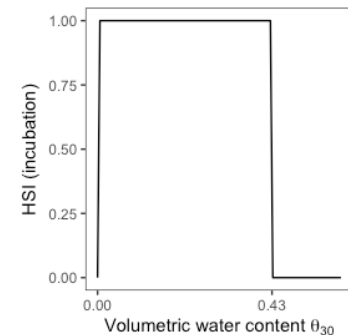
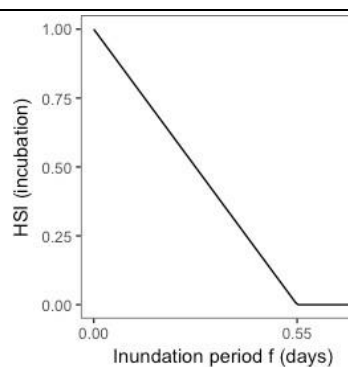
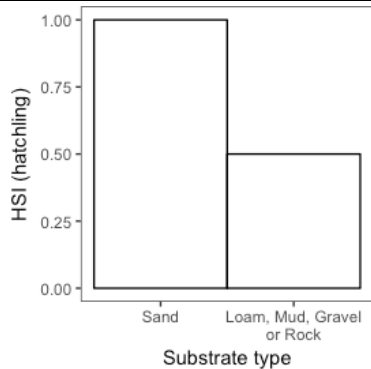
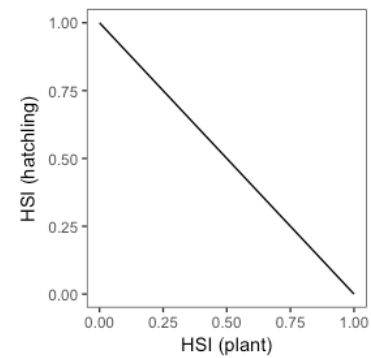
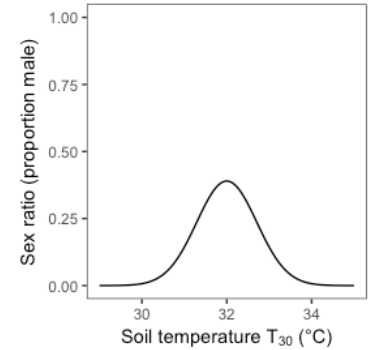
Life stage (j)	Environmental condition (i)		Habitat Suitability Index (Φ)		Rationale	Source	Comment
	h	Past peak water level during wet season inundation (meter)	Φ_{dep}^{sprout}		Resprouting becomes less likely if plant was submerged in last wet season flooding.		
	f	Period of inundation (days)	Φ_f^{sprout}				Assumed same as adult plant
	U	Inundation flow velocity (m/s)	Φ_{vel}^{sprout}		Resprouting becomes less likely if plant was subject to high flows in last wet season flooding		Critical U assumed as 5 m/s

Table 4. Habitat requirements that define the habitat index for the Australian freshwater crocodile (AFC), *Crocodylus johnstoni*.

Life stage (j)	Environmental condition (i)	Habitat Suitability Index (Φ)		Rationale	Source	Comment	
Nesting (mid-Aug–mid-Sep, nest site selection from late Jul)	Sub	Substrate type	Φ_{sub}^{nest}		Nesting females prefer friable, sandy substrate for ease of nest excavation	Somaweera and Shine (2013)	
	θ_{20}	Soil volumetric water content at 20 cm depth	Φ_{vwc}^{nest}		Females select moist but not saturated (or overly damp) soil. 20 cm is an approximate mid-nest depth (WA Ord river, Somaweera & Shine 2013).	Somaweera and Shine (2013)	0.43 assumed. Ord riverbank nests 0.014 <= 23 <= 0.266 (converted from gravimetric assume bulk density=1.4) Somaweera and Shine (2013)
	P	Potential presence of <i>P. foetida</i>	Φ_{pss}^{nest}		Densely vegetated sites restrict nesting	Smith (1987)	

Life stage (j)	Environmental condition (i)		Habitat Suitability Index (Φ)	Rationale	Source	Comment	
Egg incubation (mid-Aug–early Nov)	T_{20}	Soil temperature at 20 cm depth (°C)	Φ_{tem}^{inc}		Incubation temperature profoundly influences embryonic development rate and hatchling size	Webb et al. (1987), Lang and Andrews (1994)	
	θ_{20}	Soil volumetric water content at 20 cm depth	Φ_{vwc}^{inc}		Embryo mortality increases in both overly dry and overly wet soils	Webb et al. (1983), Mazzotti (1989)	Ord riverbank nests 0.014 ≤ 23 ≤ 0.266 (converted from gravimetric) Somaweera and Shine (2013)
	f	Period of inundation (days)	Φ_f^{inc}		In related species (<i>C. porosus</i>), 13 hours of submission in water kills all eggs	Magnusson (1982)	

Life stage (j)	Environmental condition (i)		Habitat Suitability Index (Φ)	Rationale	Source	Comment
Hatchling success (Nov–Dec)	Sub	Substrate type	Φ_{sub}^{hatch}			
	P	Potential presence of <i>P. foetida</i>	Φ_{pss}^{hatch}		Nest emerging may not take place if nest is completely covered by <i>P. foetida</i>	Somaweera (pers. comm.)
Sex ratio (proportion male)	T_{20} or Degree days	Soil temperature at 20 cm depth ($^{\circ}\text{C}$)	Φ_{tem}^{male}		Males are only produced at intermediate temperatures. Maximum proportion of male (0.39) is reached at a constant incubation temperature of 32°C. Thermosensitive period is day 35–42 at intermediate temperatures.	Empirical data: Webb et al. (1987), Lang and Andrews (1994) TDSD reaction norm: Somaweera et al. (2019)

3. Danggu (Geike Gorge) application and data requirements

The model is applied to Danggu (Geike Gorge) National Park with a focus on resolving the river pool and sandbanks within the gorge, and making use of available data from Somaweera et al., 2020 and 2021).

The model approach described in Section 2 integrates a range of data sets that are used either for model setup or assessment. The sources of data and the integration of the various datasets with the model and associated workflow is described in Figure 5. The datasets and data preparation for the model are explained in more detail below.

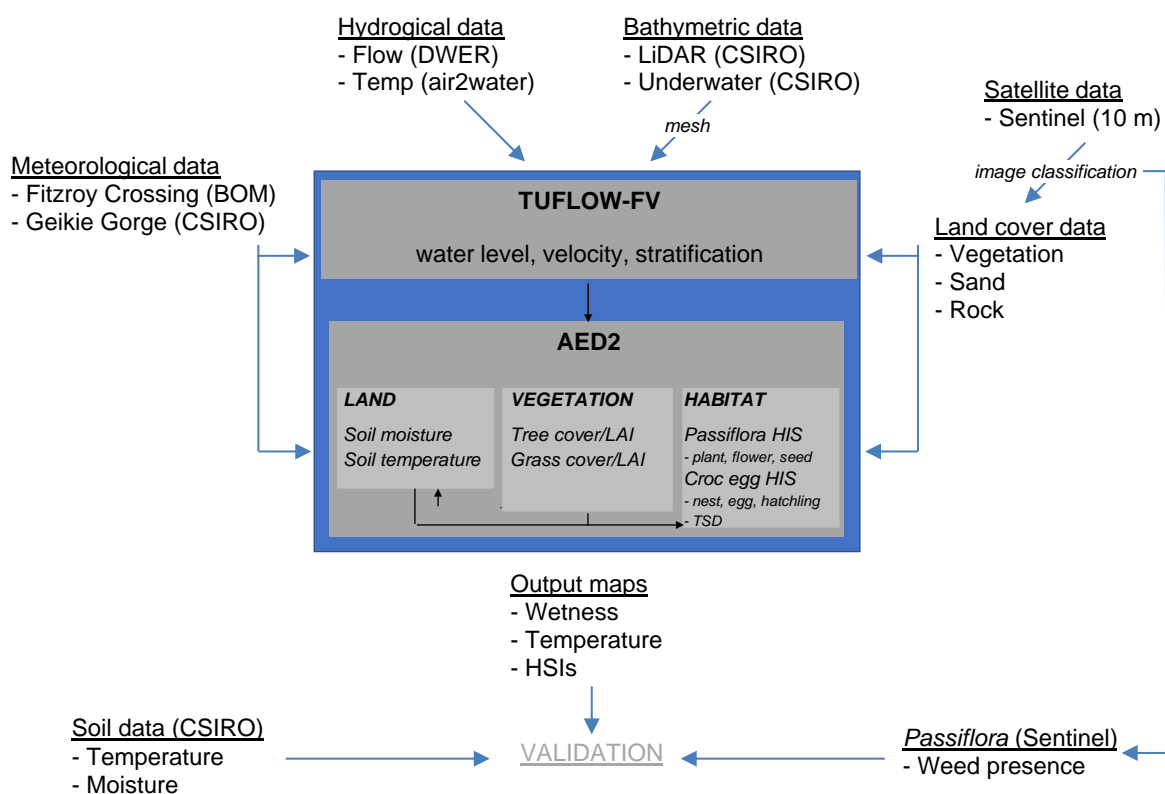


Figure 5. The integrated model approach is supported by a range of data sourced from different providers. Various data pre-processing is required to run the model, and then model outputs can also be compared with available monitoring where available.

3.1 River and floodplain morphometry and mesh generation

The river and floodplain morphometry data was derived from three sources: the CSIRO supplied LiDAR and Sonar data-sets, and the SRTM-derived 1 Second Digital Elevation Models Version 1.0 (Gallant et al., 2011).

The LiDAR data was separated out into vegetation and land rasters, then subsampled down to a 1 m resolution for further processing. Errors in the LiDAR data, mainly around the water

surface, were manually removed (Figure 6). This provided high-resolution data of the topography above the water line.

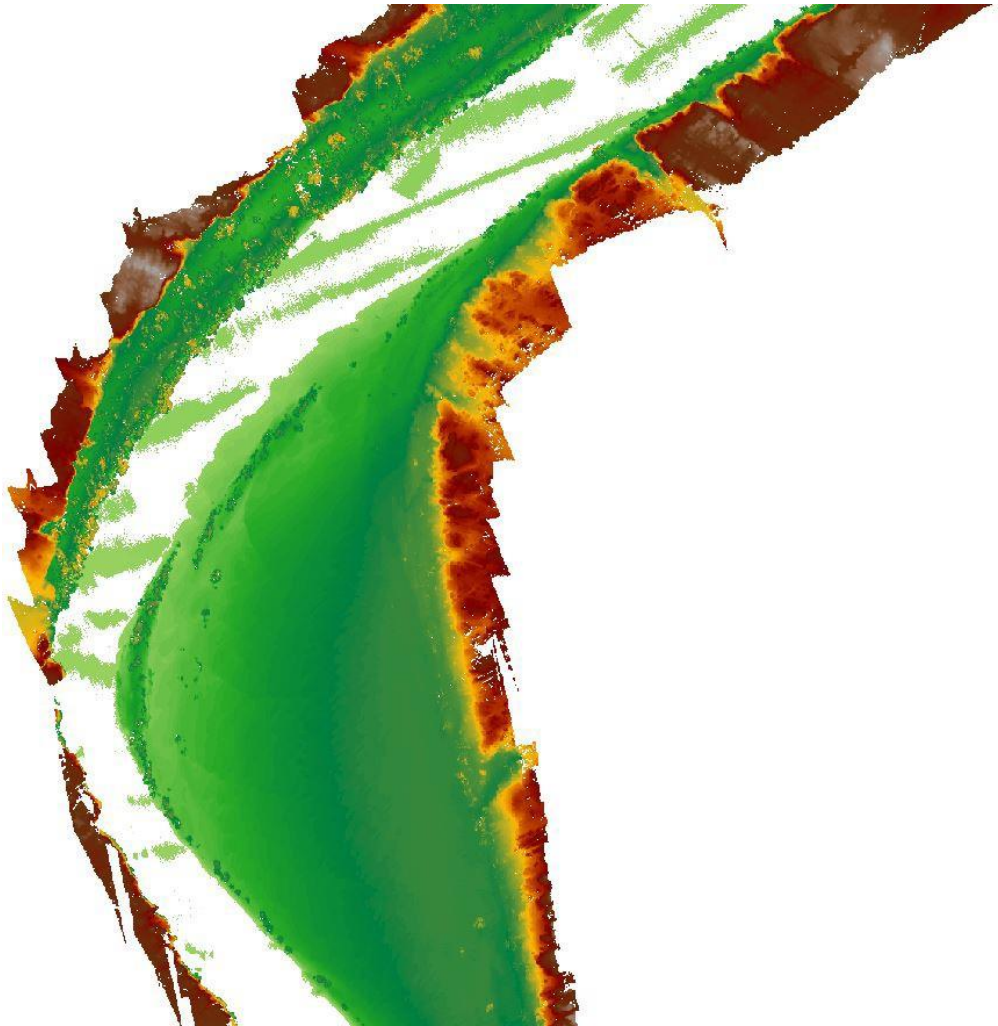


Figure 6. LiDAR data sub-sampled to 1 m resolution.

Sonar data was also collected to describe the bottom depths, below the water surface. The sonar data was post-processed using the ReefMaster software, which was then referenced to the model's datum (AHD). A small section of the domain extended beyond the Sonar's extent, which was filled with extrapolated Sonar data and use of assumed depths (Figure 7).

Portions of the simulated floodplain domain also fell outside of the LiDAR's extent. The 1-second SRTM-derived DEM was therefore relied on to infill these areas. We note however, the much coarser resolution of this data compared to the LiDAR and this will impact upon prediction accuracy also in these regions.

The flexible-mesh for the TUFLOW-FV model was then created using a merged version of the above-mentioned three datasets. The mesh geometry was designed using Aquaveo's SMS software (Figure 8). The final computational mesh contained 11435 cells, with an average area of 132 m², and cells ranging between 115.63 m² and 188.61 m². Figure 9 shows the final model mesh for the domain overlaid on the satellite imagery.

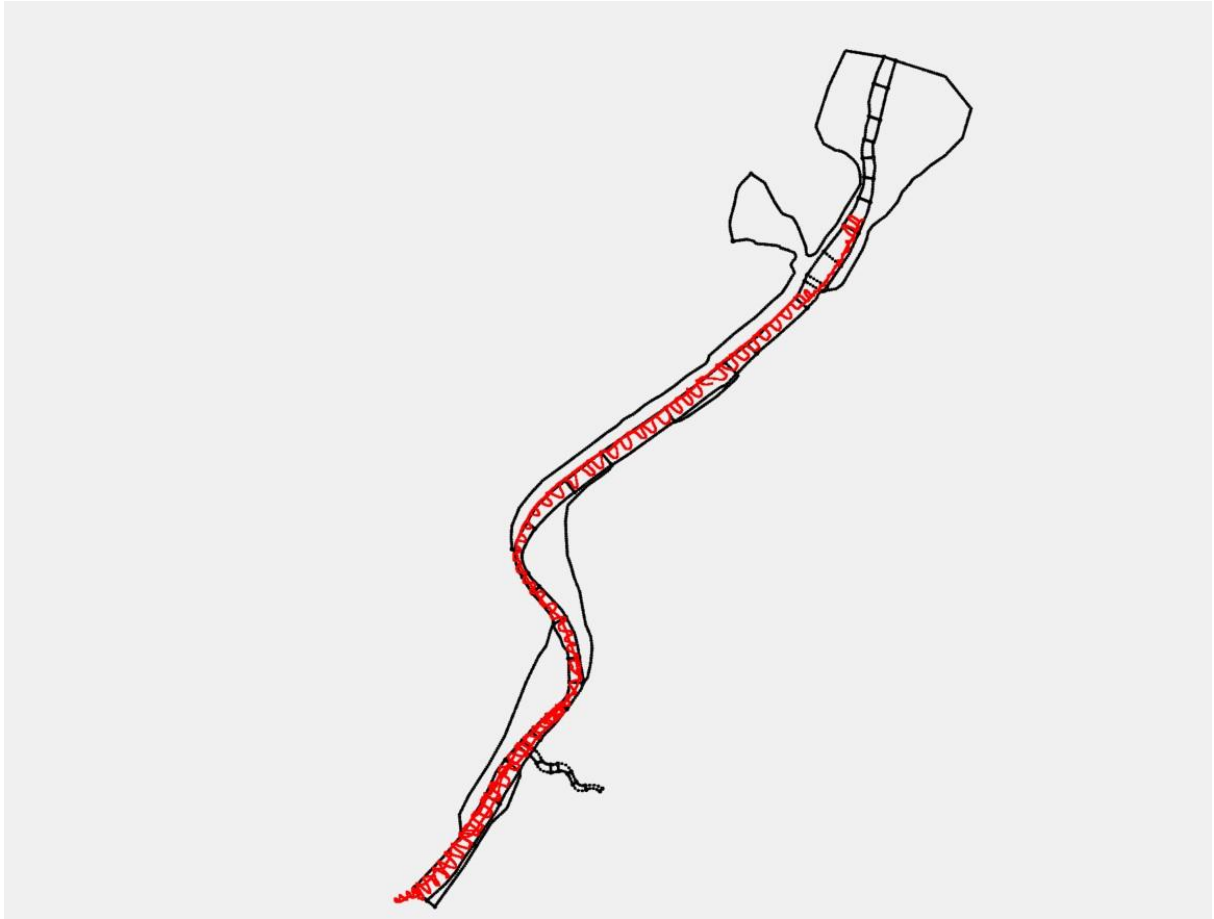


Figure 7. Sonar data track within the river channel.

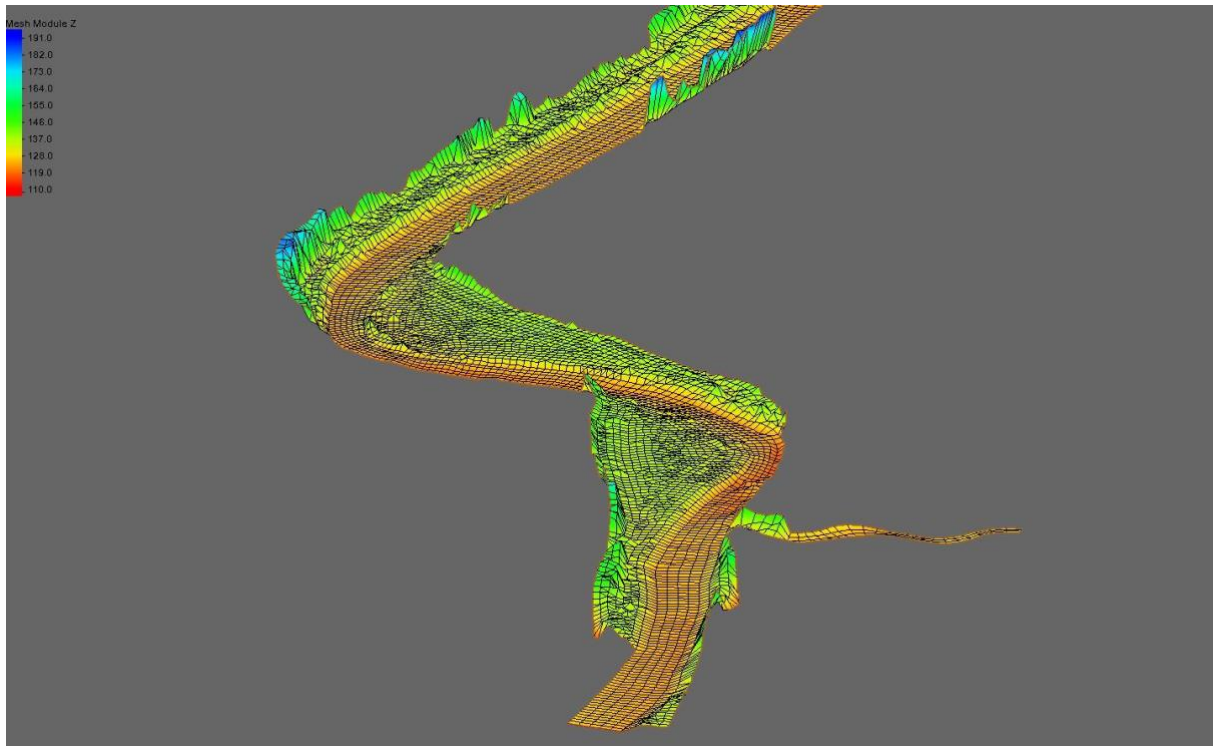


Figure 8. Example model mesh, generated after splicing of the sonar and LiDAR data.

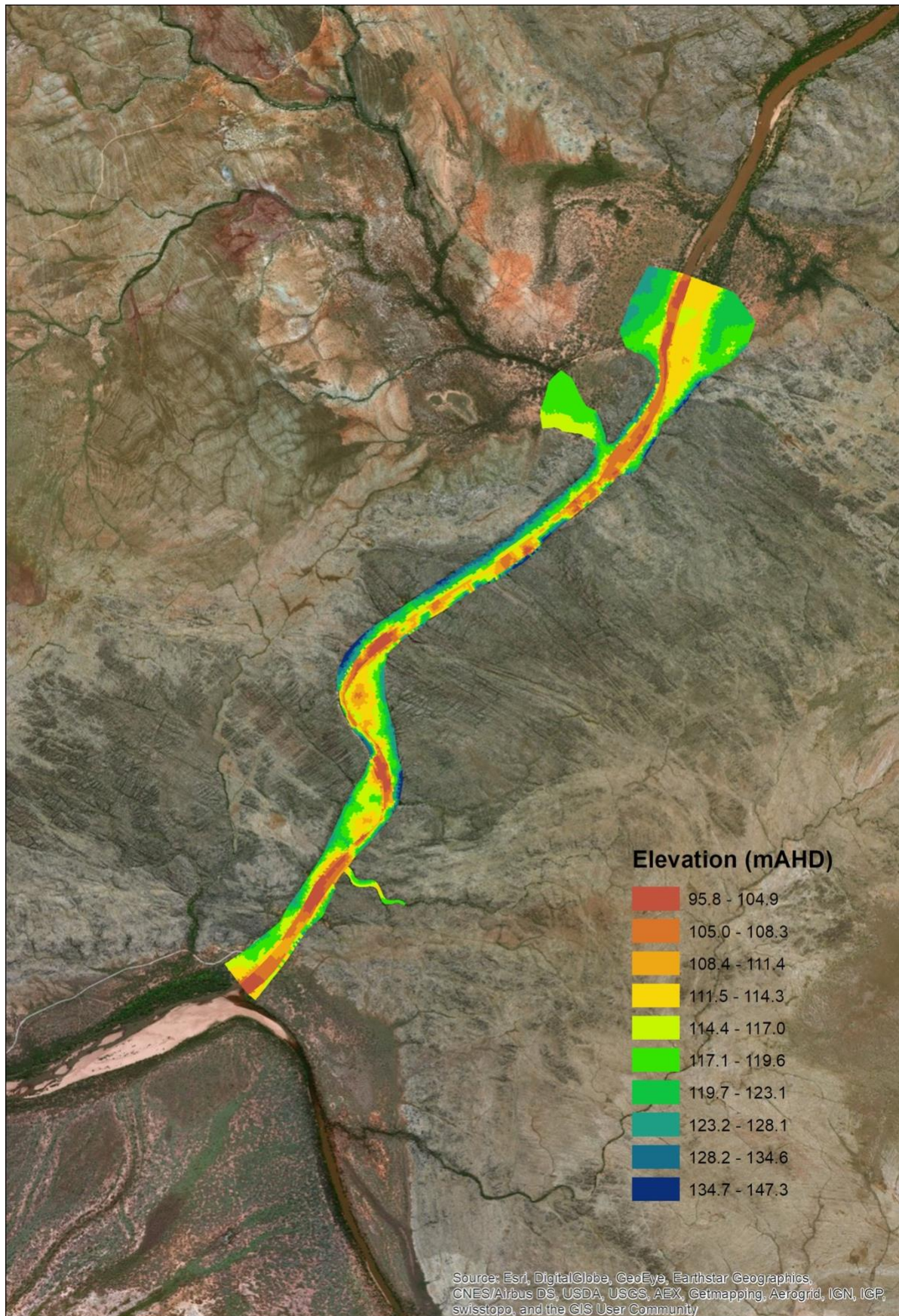


Figure 9. Final model domain created for the TUFLOW-FV – AED simulation, showing cell bottom elevations.

3.2 Land surface cover and vegetation biomass

Sentinel-2 imagery was first used to compute land-surface cover as ~10m pixels across the region. The land-types were completed using a classification training process for 5 land cover types (water, vegetation, sand, rock and *P. foetida*). A combination of several dry season images from between 2016–2018 were utilised for this. After training the final land cover results are as shown in Figure 10. There is some misclassification noted by this process, for example, on the edge of sand banks being considered as rock, when this is likely darker cells with vegetation, water and sand being incorrectly identified as rock. But overall, the dataset is a useful source of substrate information that was used as input to the coupled model.

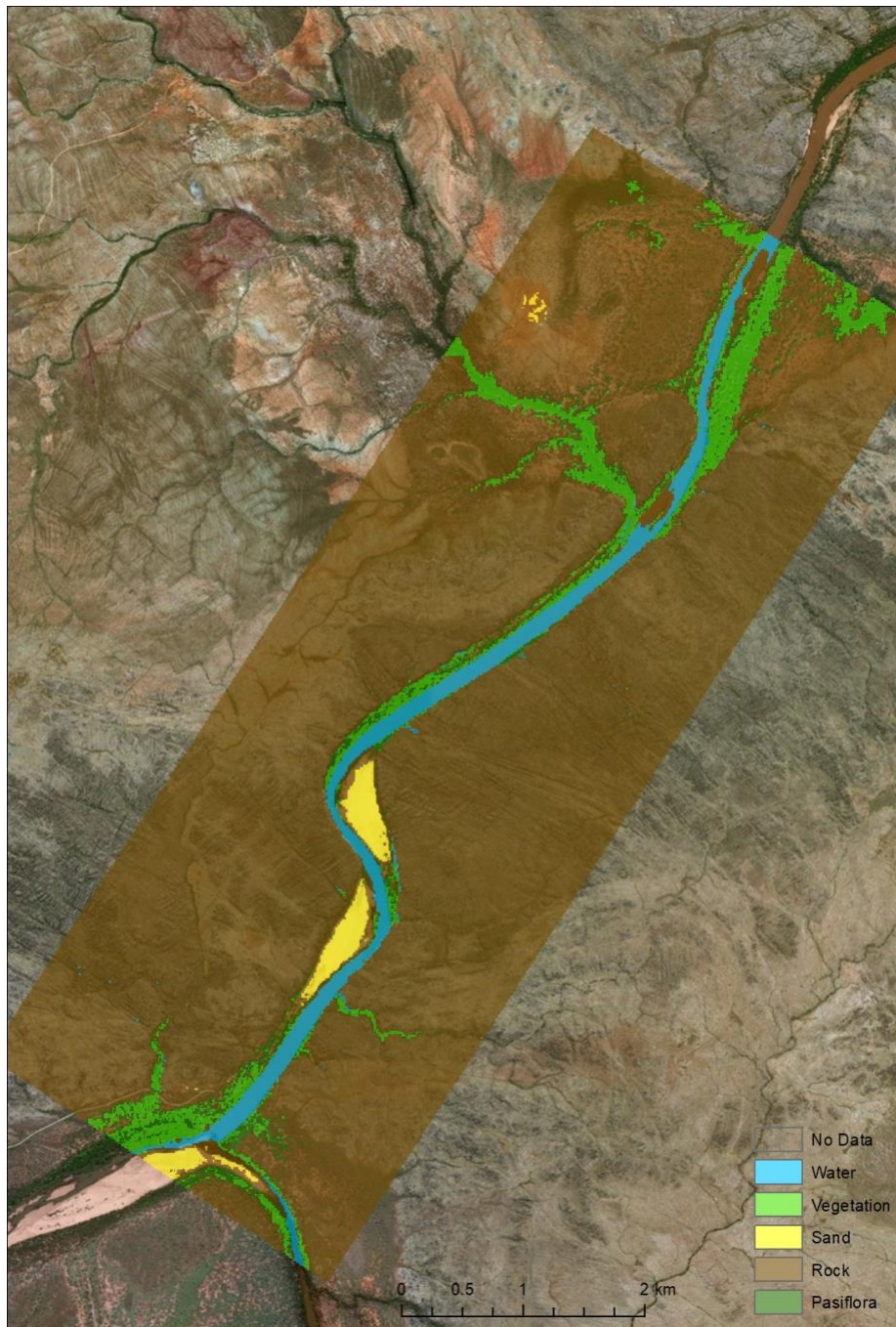


Figure 10. Identification of 5 land cover types based on a guided classification process undertaken on high-quality (cloud-free) dry-season images taken from Sentinel-2.

We then overlaid the model mesh (Figure 9) onto the land-cover classes (Figure 10) and computed in each model cell the percentage area of the five land-cover types. Figure 11 shows a sub-reach indicating the model resolution and the assumed land and vegetation conditions.

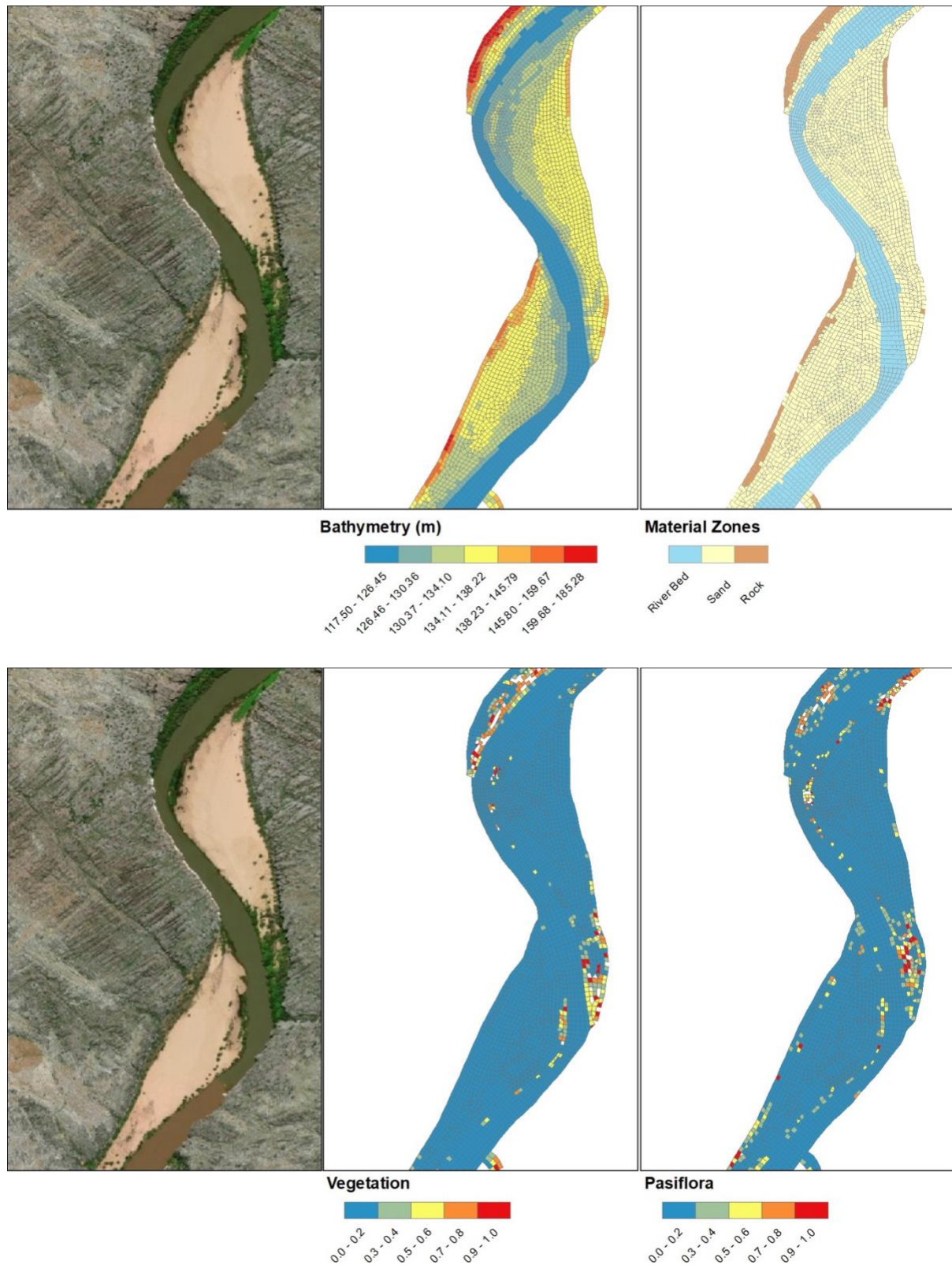


Figure 11. Sub-region plot of (a) the model mesh and cells material classification, and (b) relative cover of vegetation (area fraction).

3.3 Hydrological conditions

Hydrological data from the Department of Water and Environmental Regulation (DWER) was used to drive a typical seasonal water flow regime within the simulated Geike Gorge model domain. At the upstream boundary the flow data from station 118639 (Dimond Gorge) was used with the data retrieved from the DWER Water Information Reporting (WIR) website. At the model downstream boundary an 'open' flow condition was assumed reflecting water discharge leaving the Gorge at the Fitzroy Crossing gauge.

3.4 Meteorological conditions

Meteorological data is required to drive the soil and water thermodynamic sub-models. Hourly data were sourced from Bureau of Meteorology (BOM) station 003006 (Fitzroy Crossing) for background meteorological conditions (solar radiation, humidity, air temperature and windspeed; data not shown). For a period in 2017, local data was available in the form of two stations that were temporarily located within the study area (Figure 12). Where this data was available it was used within the model, elsewhere the BOM data was used.

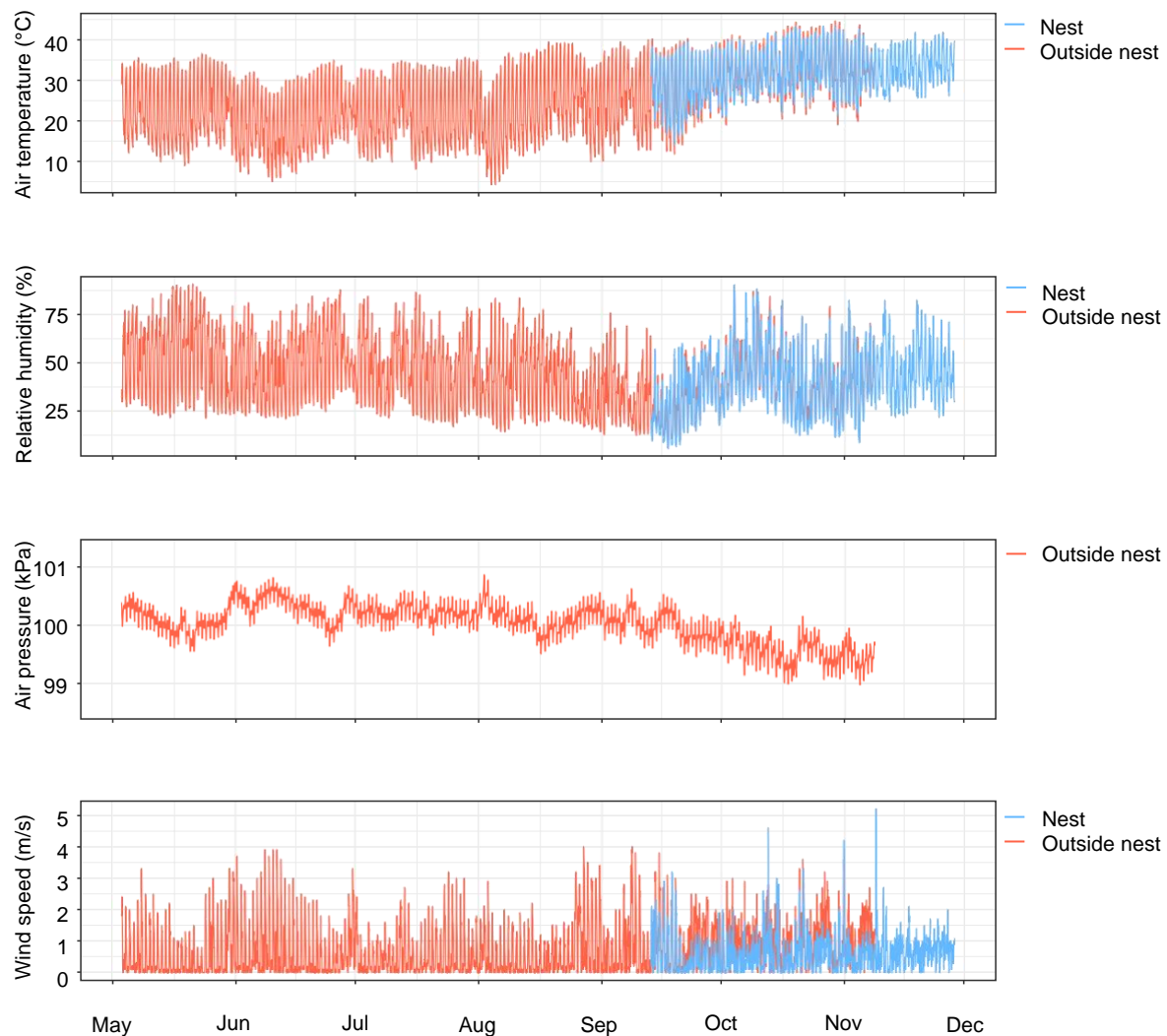


Figure 12. Local weather data collected within the Geike Gorge domain in 2017, within and outside of a nest location.

Figure 13 shows the soil moisture and temperature data provided, which was used to guide assessment of the soil model hydrological parameters. Data analysis presented in Somaweera et al. (2021), show that on average soil temperatures at 30c m depth were $\sim 2^{\circ}\text{C}$ cooler in sites with *P. foetida* over-topping the soil.

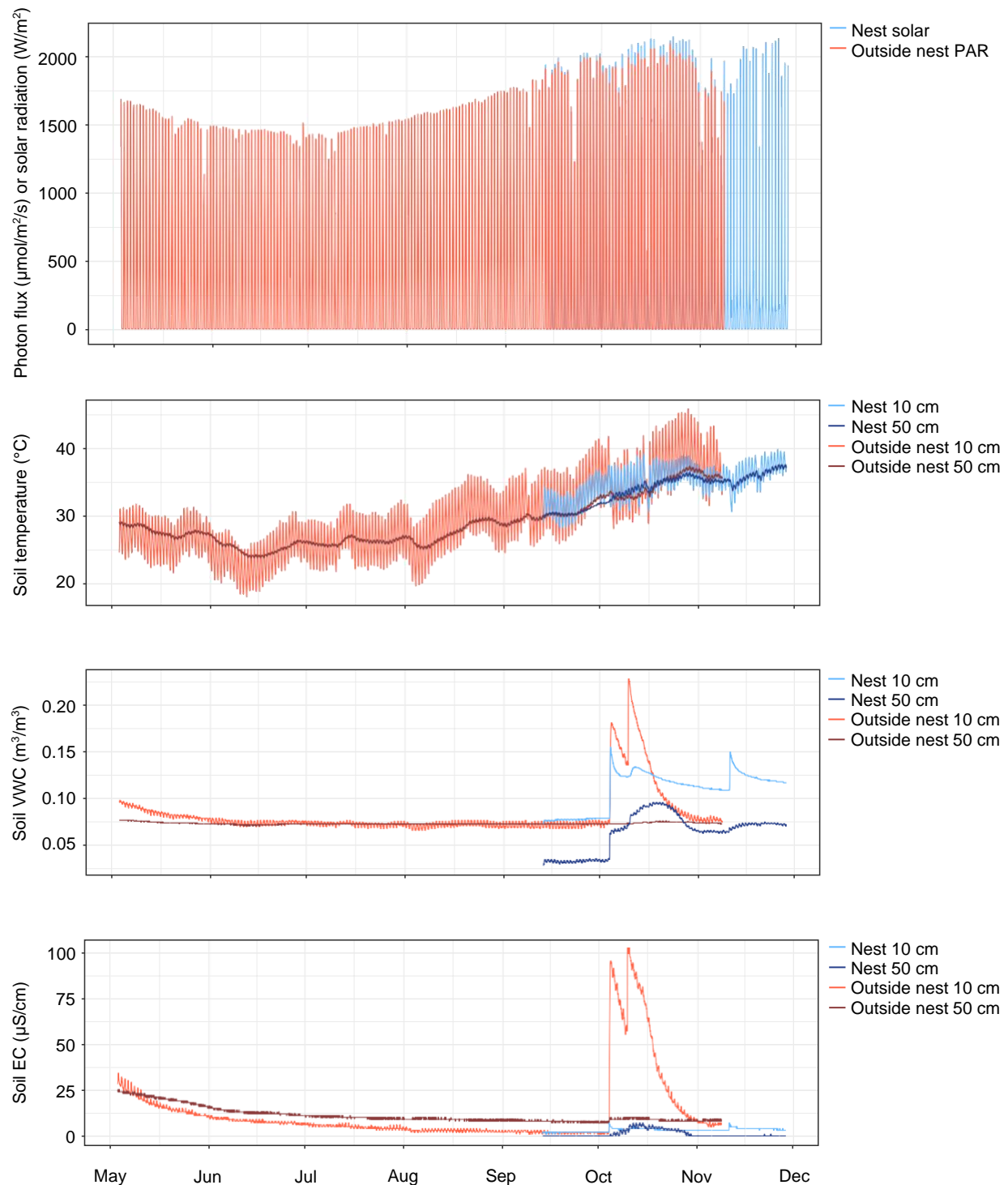


Figure 13. Local data collected within the Geike Gorge domain in 2017, within and outside of a nest.

The above data were used to estimate the soil hydraulic parameters used within the model substrate class of sand, such as the field capacity.

4. Model results

4.1 River hydrology

Simulations were undertaken with a range of adjustments to the hydraulic conditions to capture the flow pulse dynamics, and subsequent water level recession. Data from the Dimond Gorge and Fitzroy Crossing gauging stations were compared with the water level variation predicted from the model (Figure 14). Unfortunately, no water temperature data was available, though in general the seasonal changes predicted seemed within a reasonable range. The model captured the flow peaks well but underpredicted the recession of the water level in the drier months, which is assumed to be related to poor specification of the hydraulic conditions near the domain outlet (related to the cease-to-flow (CTF) elevation and rating error) rather than error in the pool bathymetry. Alternatively, it may be due to lack of groundwater exchange, or errors in the rate of evapotranspiration causing the model to overpredict the depth of water pooling in the gorge. However, given the limited data and focus of this project the hydrology was kept simple and further refine of the hydrologic dynamics is left for further refinement.

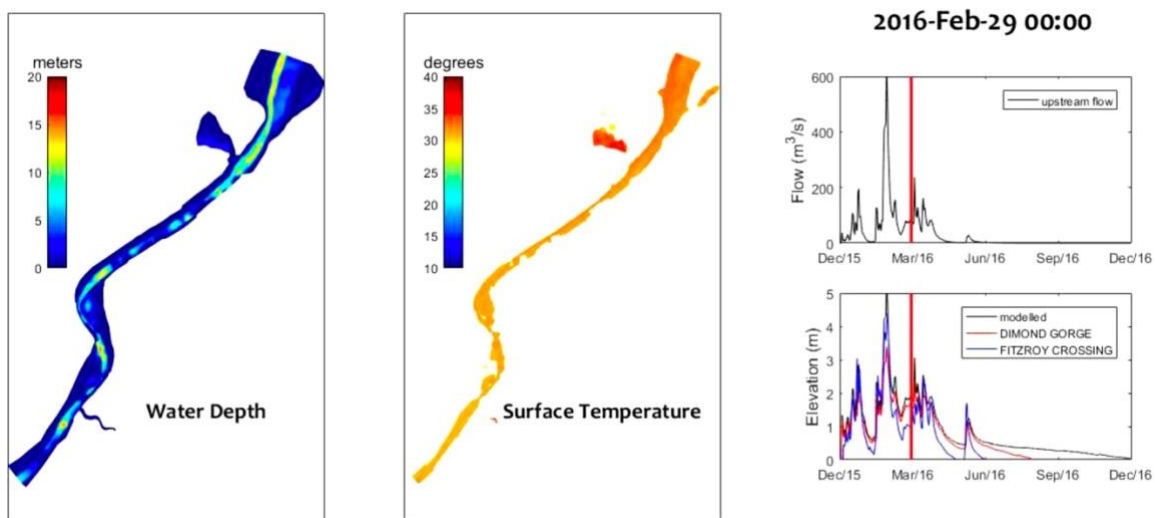


Figure 14. Example output from the hydrodynamic model, compared with observed flow data (bottom right inset).

4.2 Soil dynamics

An example of the soil temperature and moisture dynamics near the water's edge contrasted against conditions further away from the river channel is shown in Figure 15. The results show the diurnal heating and cooling of the soil, responding to air temperature and solar radiation changes. It is also possible to see the periodic effect of rain events causing surficial soil moisture increases, which are then followed by a period of drainage, whereby the soil moisture moves downward as a wetting front. In exposed areas (not shaded by vegetation), the soil becomes very dry in top 25 cm, particularly between April and July, and temperatures exceed 35 °C during the day. The prediction at the 10 cm depth matches well the measured data mean and range shown in Figure 13, noting the model is in 2016 and the field data was

measured in 2017. The measured data for soil moisture (also in Figure 13) shows dry conditions tend to be ~ 0.08 (v/v), which matches the model during a similar dry period.

As the model accounts for vegetation shading and water use, cells that are in vegetated areas are generally shown to be cooler due to less incident sunlight, and they have higher moisture. This is despite the extra water use by the plants, at least based on the default parameters used in the model in this case. Overall, it was not possible to do a detailed calibration of the soil model temperature and moisture with the field data available, but the model does appear to give indicative and realistic values for the purposes of demonstrating the modelling approach.

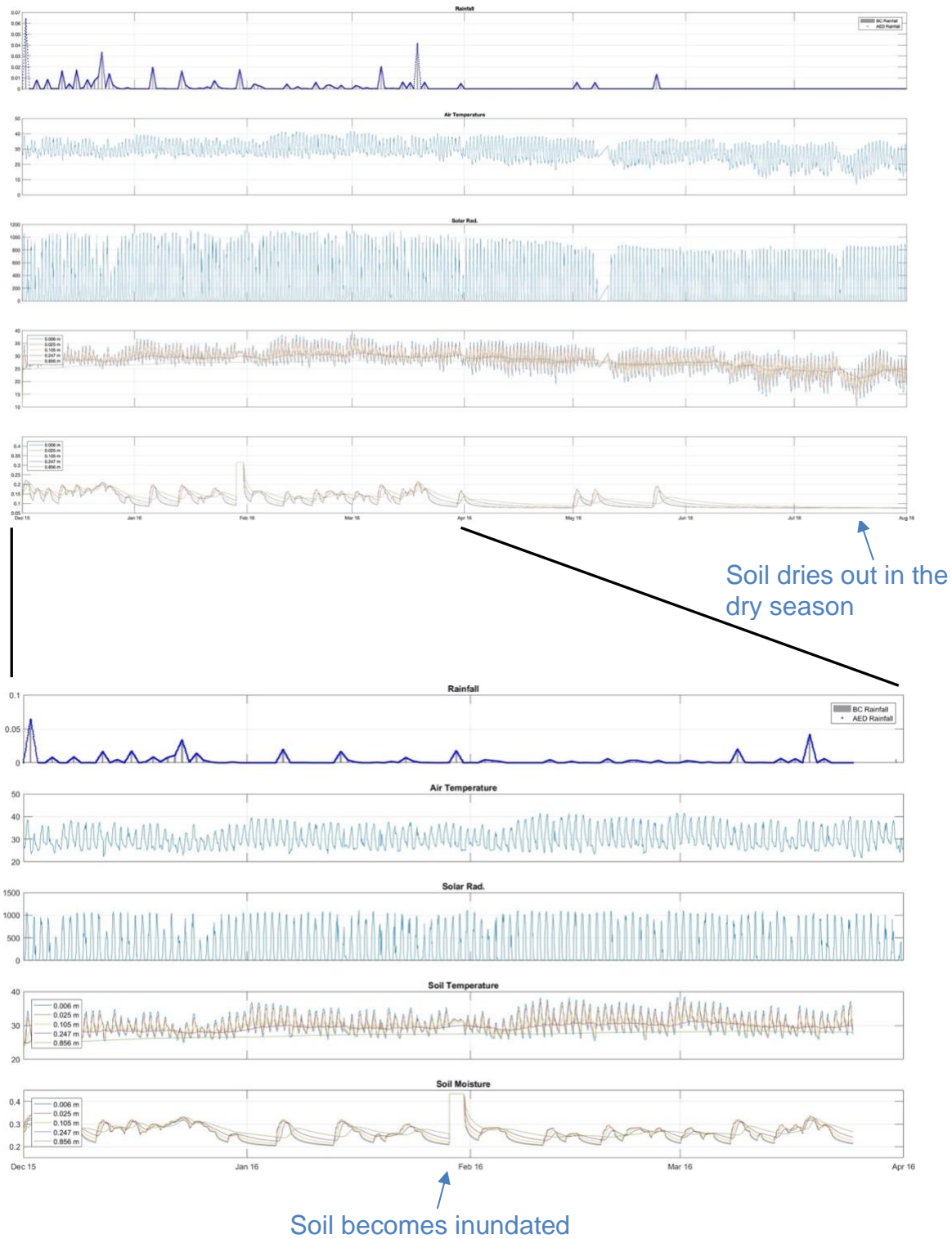


Figure 15. Example output from the ecohydrology model for a chosen cell, showing the long-term meteorological drivers of soil temperature and soil moisture (VWC). The bottom panel set is shown over a zoomed time window to highlight the vertical changes in soil moisture following rainfall inputs, and the timescale of downward drainage.

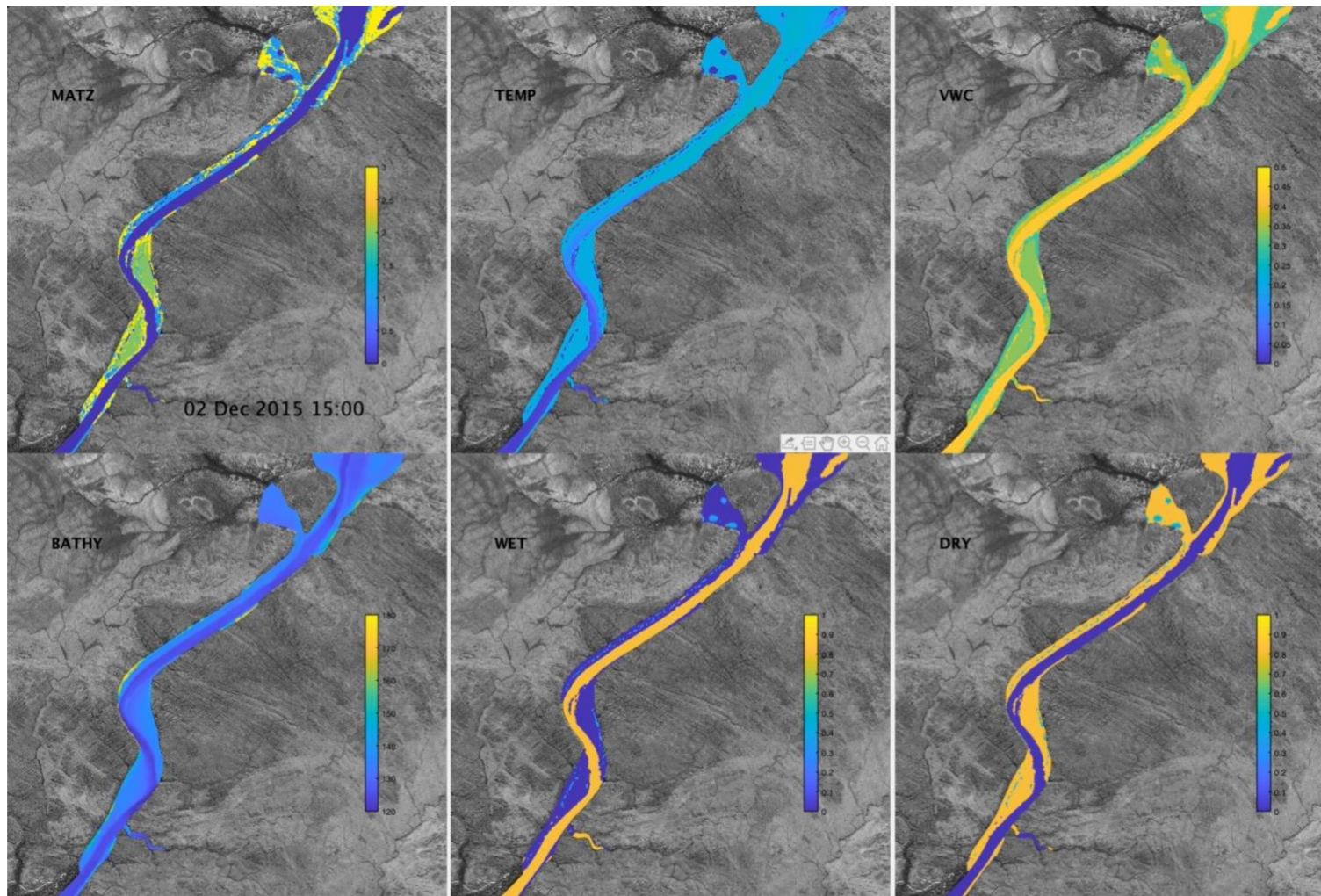


Figure 16. Example output from the ecohydrology model showing the spatial predictions of the model substrate (MATZ), temperature (water or soil surface), soil moisture (VWC), bathymetry (BATHY), and the wetime (WET) and drytime (DRY) outputs.

4.3 Habitat suitability: *Passiflora foetida*

The model predicts the overall habitat condition, 'HSI', representing adult growth, resprouting likelihood, and seedling establishment, based on sensitivity to the various environmental factors – as denoted by the Φ functions. HSI maps for each of these life-stage categories and the associated contributing environmental functions are shown below (Figure 17, Figure 18 and Figure 19).

For the conditions simulated within 2016, the adult plant growth conditions were predicted to have a relatively low index value overall (between March to July), due to the main constraint based on insufficient soil moisture, which was on average below the optimal requirement that was specified in Table 3. As a result, the plant suitability overall was predicted to be <0.3 for the main growth period. On assessing this, it is difficult to ascertain if the model is underpredicting soil moisture from the data available; it could be the model is underpredicting soil moisture, which would lead to an overall low score, though it is noted that 2016 was a relatively low flow year, and was characterised by dry conditions over the averaging time.

For seedling establishment, the overall seedling HSI similarly had low scores on average (~ 0.3), though in this case the soil moisture over the period of interest for this life-stage was high, but the temperature function became the limiting factor. This is because the specified requirement was for air temperatures above 32°C , which did not occur continuously over the focus period for this life stage (see Figure 15).

The sprout function showed a more heterogeneous pattern and reflects the combination of past plant presence (a requirement increasing the likelihood of sprouting) and environmental conditions over the averaged period, though generally the available temperature and moisture were within the optimal range. Hydrologic conditions in the latter stage of the wet season were not sufficient to remove previously active cells for *P. foetida* presence (i.e., Φ_{vel}^{sprout} was not triggered to reduce sprouting likelihood in many areas). More substantial flooding and higher floodplain velocities however would therefore more significantly reduce the spatial extent of area suitable for sprouting. This aspect of the model is somewhat idealised and local scale factors influence how well the plant is anchored and subject erosive forces will impact upon the sprouting density in reality, and further calibration and fitting of the proposed functions will help to make these predictions fit with observations.

Bearing the limitations in mind, as a general test of the HSI method, the average of the three SP life-stage HSIs was correlated with the *P. foetida* coverage data estimated from the classification of the Sentinel imagery (Figure 20). The results show a modest correlation and is reasonable noting the timeframe used in the imagery classification does not directly match the modelled period, and noting that the HSI is only indicating habitat suitability and not accounting for other local or biotic factors controlling biomass establishment. Nonetheless, the correlation with the spatial pattern between the model and imagery suggests the underlying assumptions and approach to index calculation are valid.

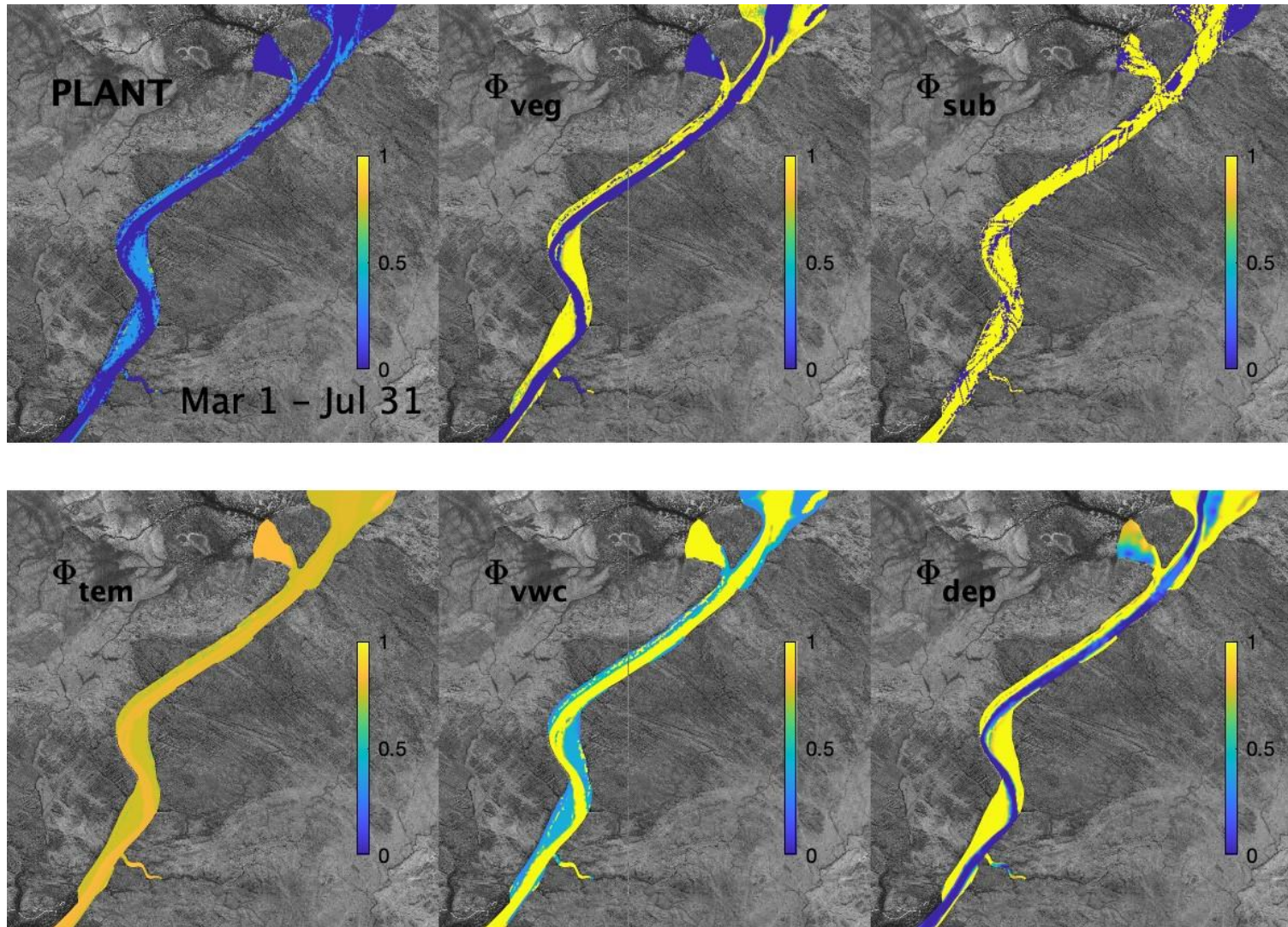


Figure 17. Output from the habitat model for 2016 conditions showing variability in environmental factors contributing to SP adult plant growth, based on average conditions throughout the relevant period (March to July).

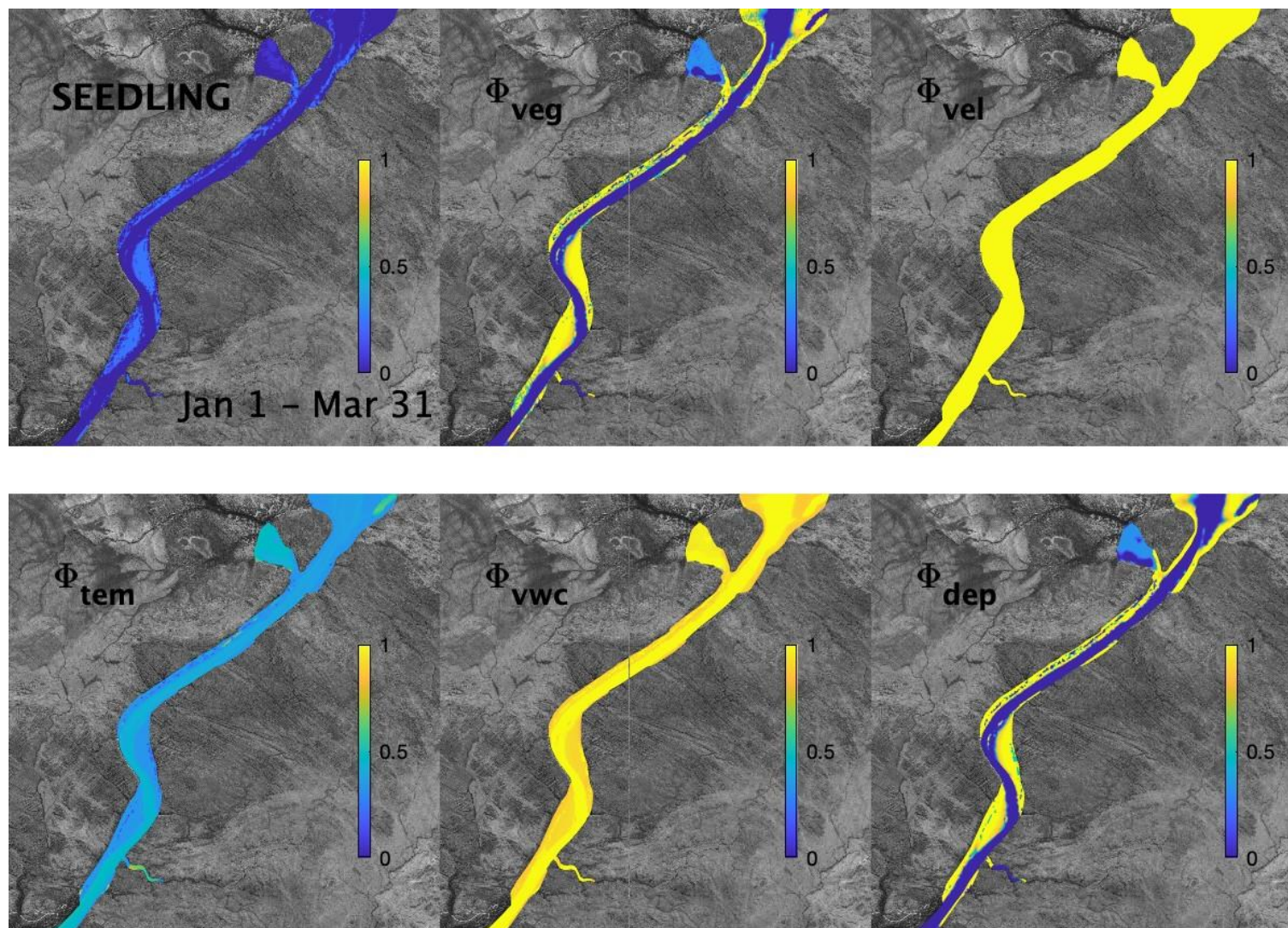


Figure 18. Output from the habitat model for 2016 conditions showing variability in environmental factors contributing to SP seedling establishment, based on average conditions throughout the relevant period (January to March).

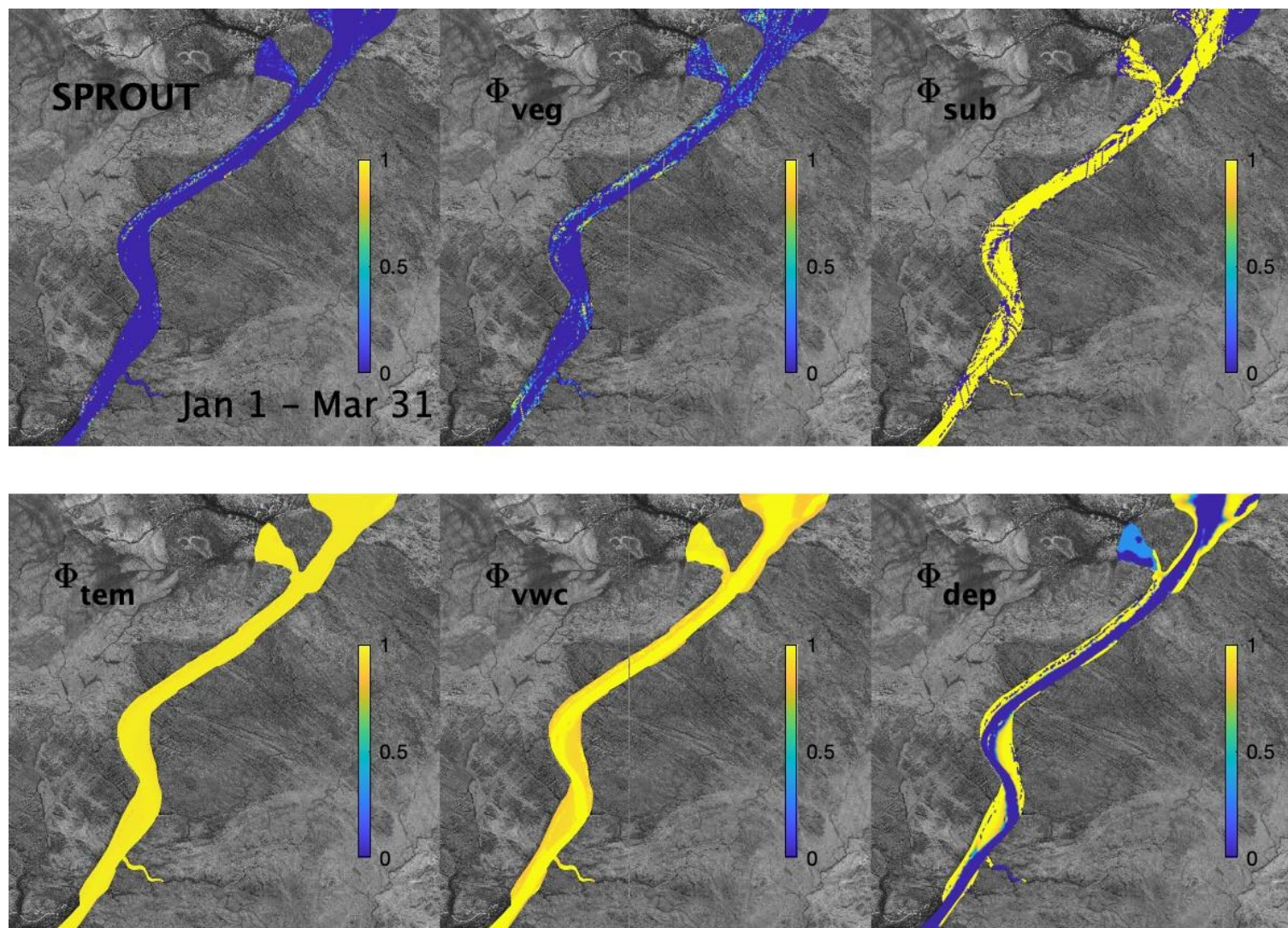


Figure 19. Output from the habitat model for 2016 conditions showing variability in environmental factors contributing to SP resprouting likelihood, based on conditions throughout the relevant averaging period (January to March).

Passiflora validation

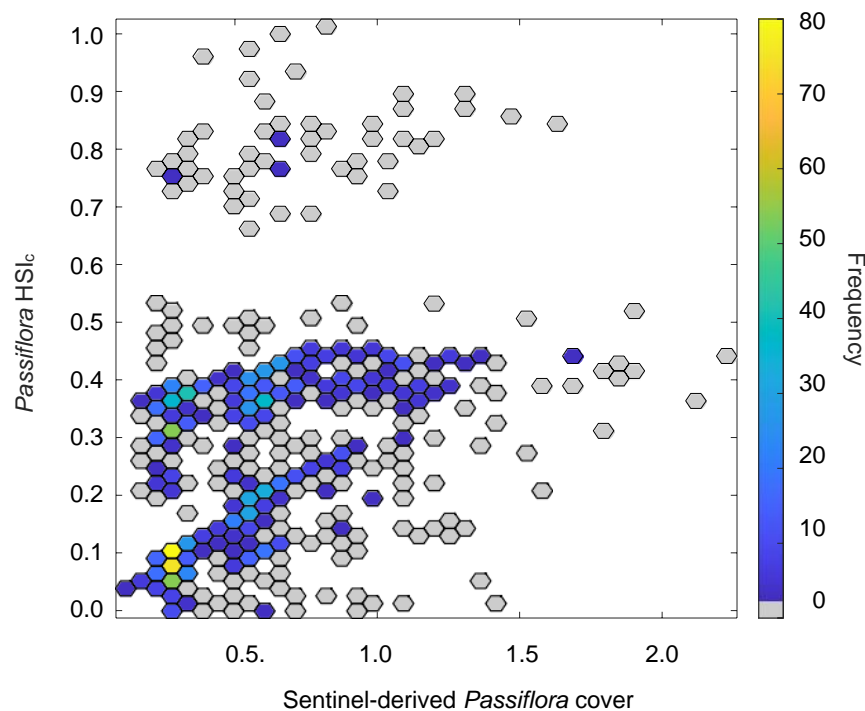


Figure 20. Comparison of composite HSI values for *Passiflora* (mean of SP HSI for the plant, sprout and seed life-stages) and the Sentinel-estimated *Passiflora* coverage data (based on the Sentinel classification, see Figure 10). Each cell is treated as a data point, though cells in the domain considered to be permanently water or rock were excluded from the correlation. The colour indicates the number of cells (frequency) reported at a particular value.

4.4 Habitat suitability: Crocodile nesting

The HSIs for AFC nesting, egg incubation and hatchling life-stage windows are shown in Figure 21, Figure 22 and Figure 23 along with the environmental factors for each as denoted by the Φ functions. The largest continuous areas suitable for nesting were predicted to be the sandy banks around the river meander. Other areas where the substrate was deemed as suitable (i.e., sandy) and within proximity to water were shown as suitable. Some inaccuracies in the substrate classification (from the Sentinel imagery) makes these areas appear slightly more patchy than would be expected, and improving the substrate classification through on-ground survey would help to prevent this source of uncertainty. The presence of *P. foetida* and dense vegetation in particular areas reduced some otherwise potential habitat (see also Section 4.5).

For the simulated period, the egg incubation HSI was highest in cells that remained dry over the averaging period, with some heterogeneity due to different temperatures across the domain. The predicted differences in temperature however were quite minor, reflecting the fact that the deeper soil temperature is used to compute this factor, T_{20} , and temperatures at this depth are less sensitive to the surface meteorological conditions, including air temperature (e.g., see 0.247 m depth in Figure 15). The small differences seen can be attributed to the effect of shading by trees canopies and *P. foetida*, reducing the incident light at the soil surface.

The hatchling success HSI predictions are controlled predominantly by the distance from water, and the presence of *P. foetida*. The geomorphology differences within the domain create different patterns of suitable areas, for example, a thin margin on the river's edge, or more substantive areas in the sandy banks.

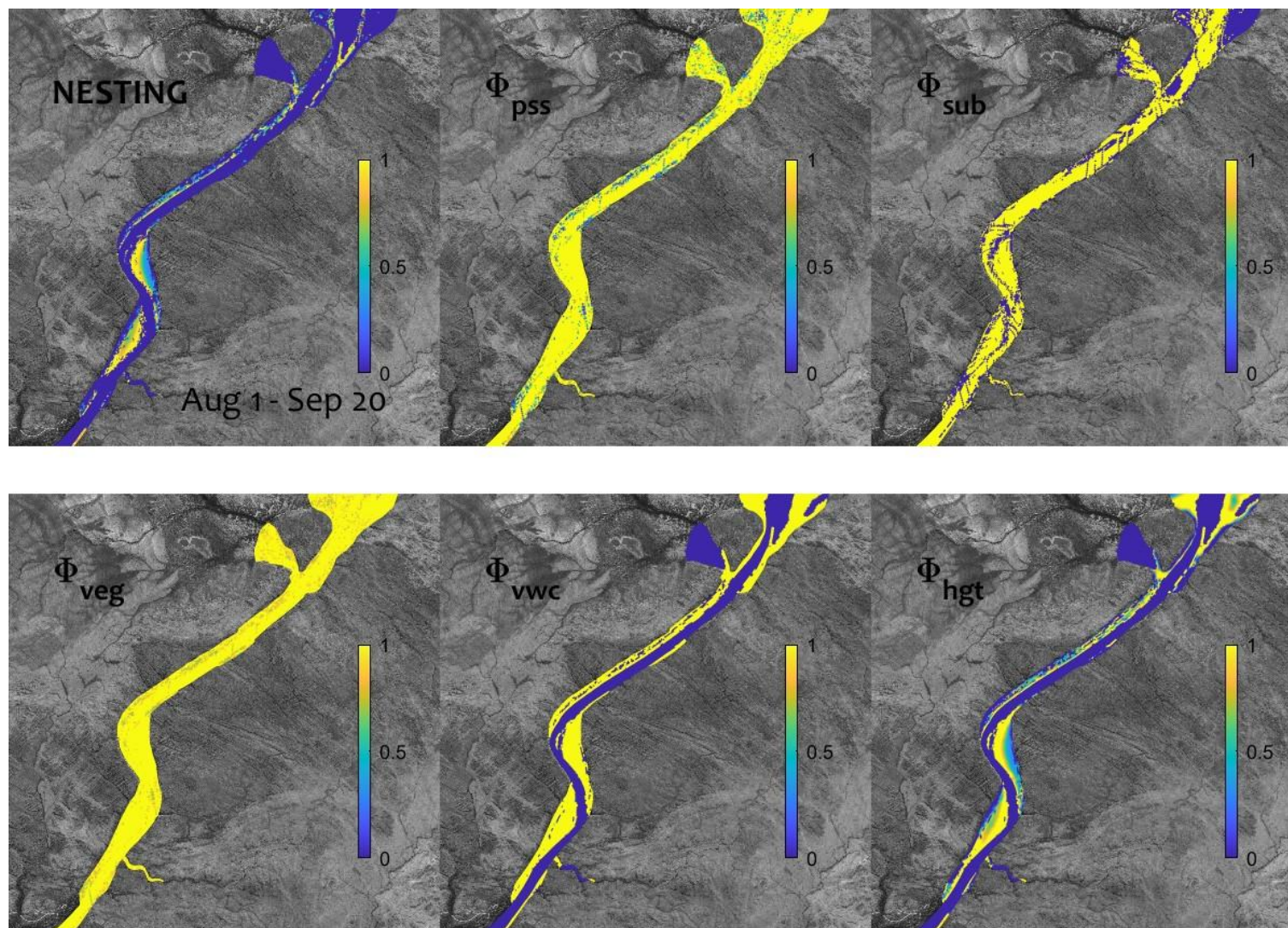


Figure 21. Output from the habitat model for 2016 conditions showing variability in environmental factors contributing to AFC nesting habitat, based on average conditions throughout the relevant period (March to July).

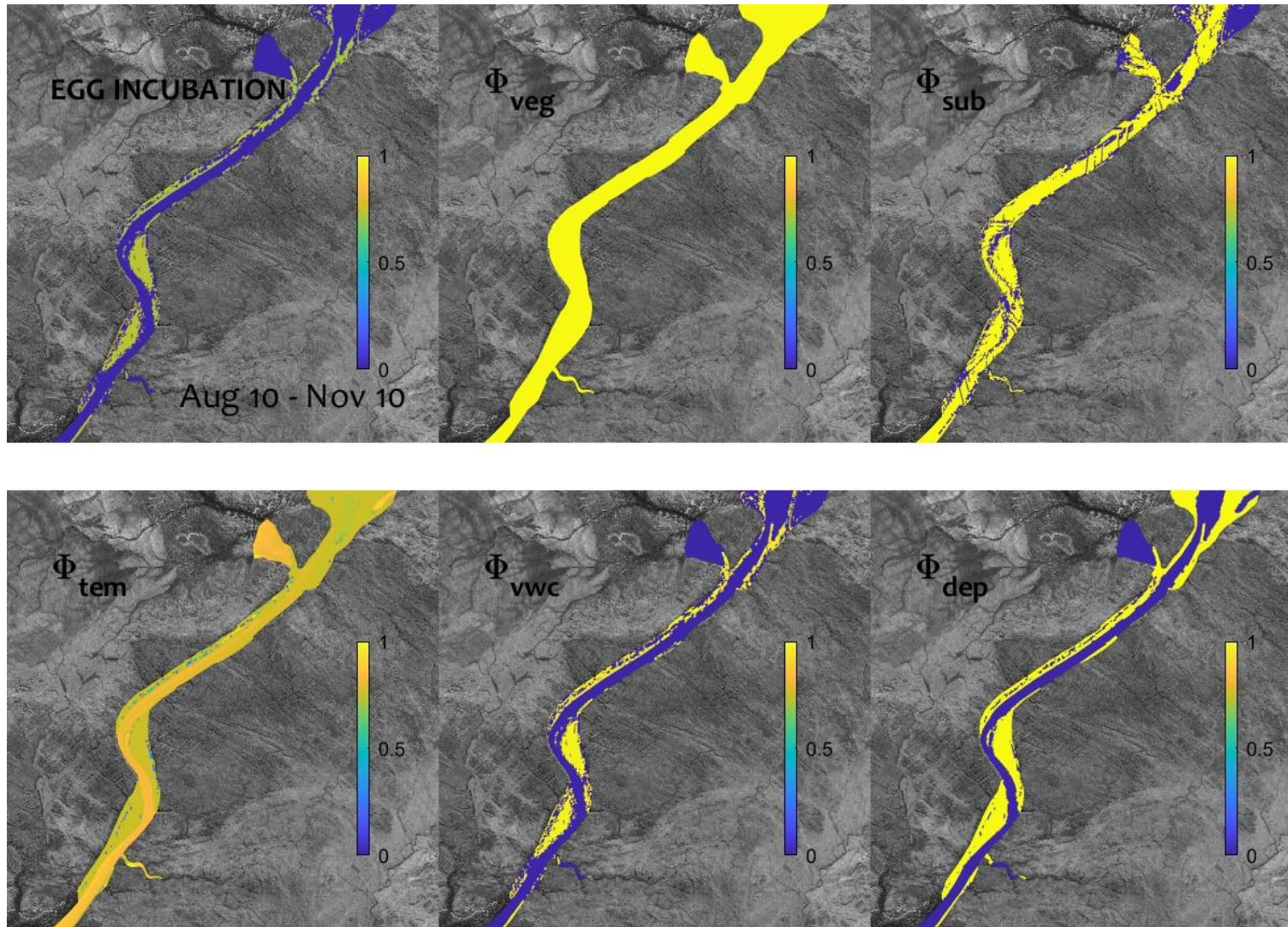


Figure 22. Output from the habitat model for 2016 conditions showing variability in environmental factors contributing to SP seedling establishment, based on average conditions throughout the relevant period (January to March).

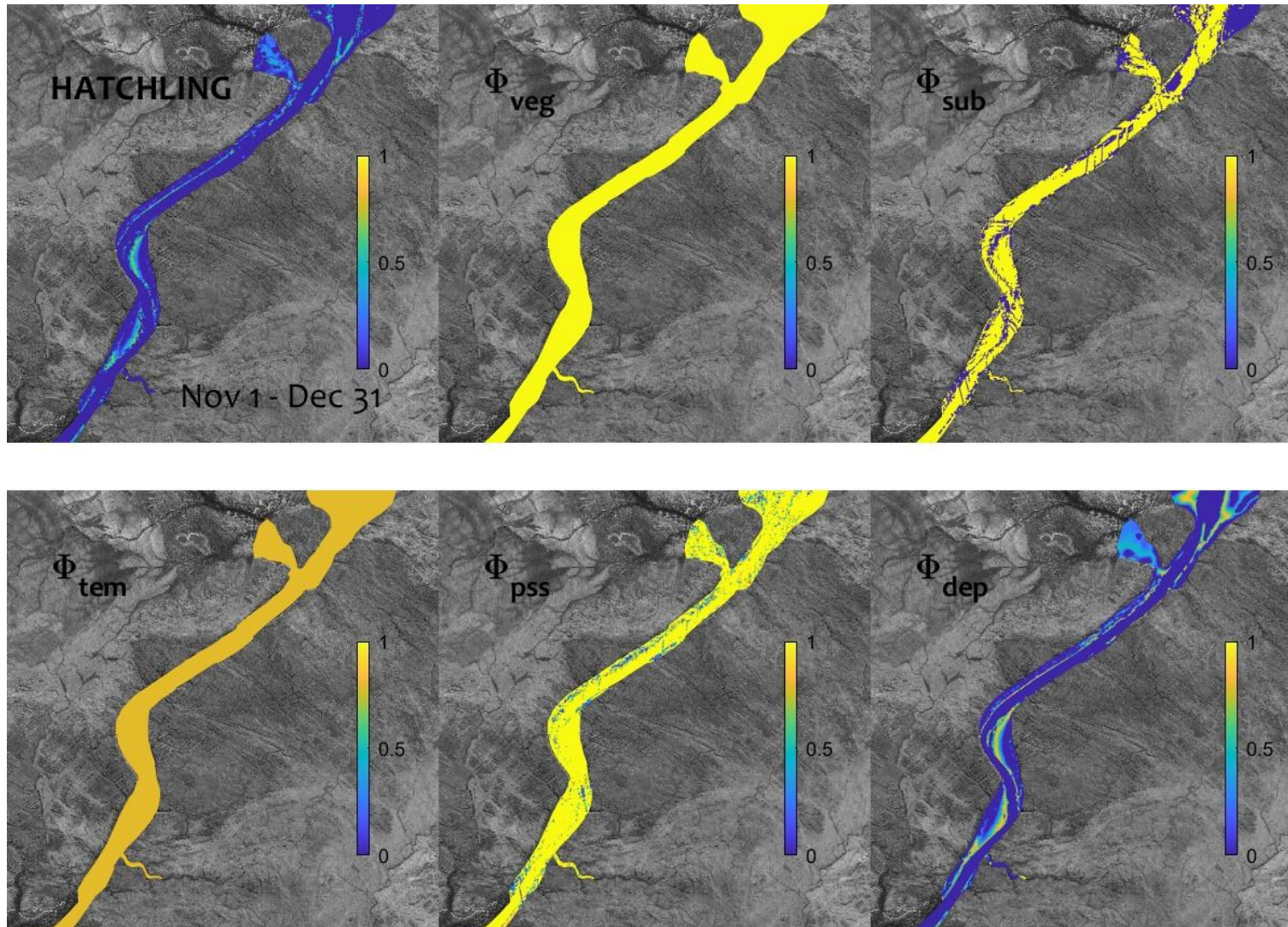


Figure 23. Output from the habitat model for 2016 conditions showing variability in environmental factors contributing to SP resprouting likelihood, based on average conditions throughout the relevant period (January to March).

The HSI for AFC nesting was compared with the known nest sites for 2016 (Figure 24). All the five identified nests occurred in areas where the nesting HSI had clusters of cells predicting values of ~ 1 . Whilst it is difficult to fully validate the HSI, noting the model refers to the potentially suitable habitat and doesn't account for population or ecological controls on nesting, the broad agreement in occurrence provides assurance the method is not misclassifying cells.

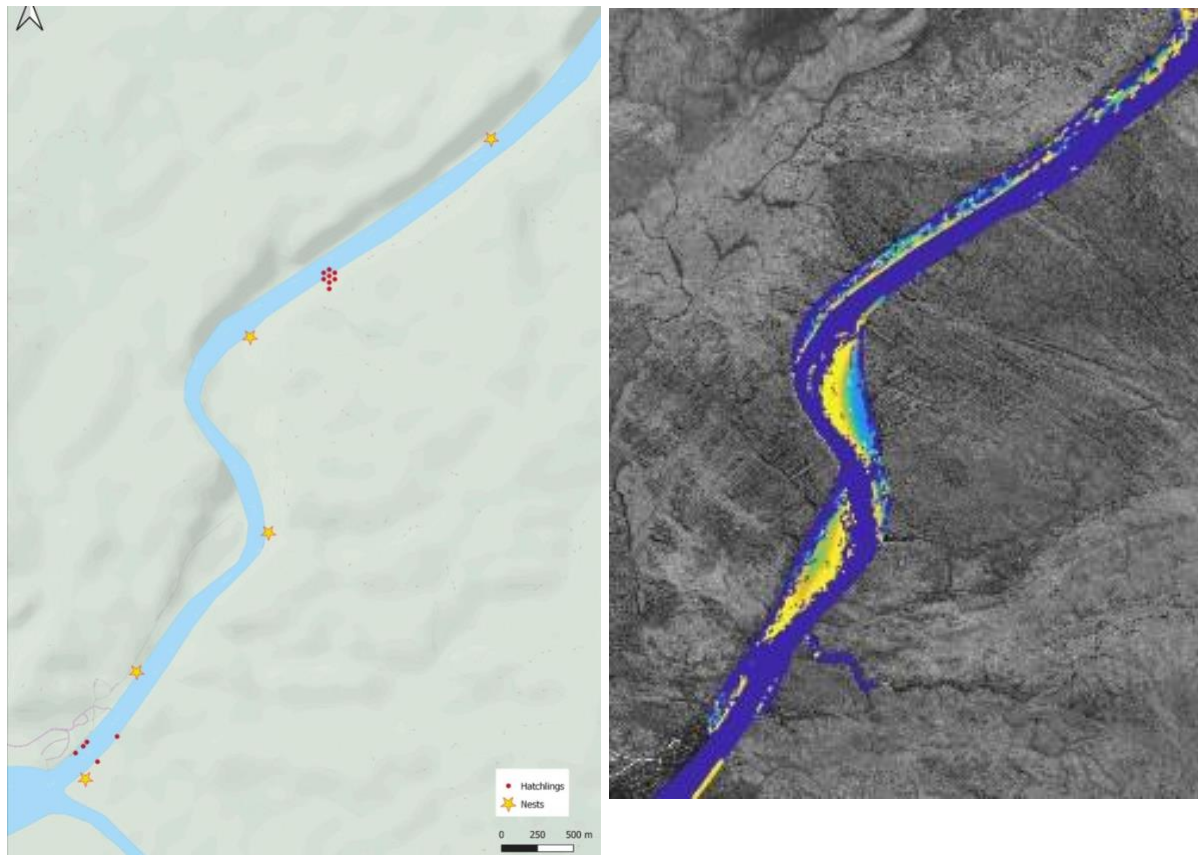


Figure 24. Monitoring data from Somaweera et al. (2021), left, showing identified nests and hatchling occurrence in the 2016 dry season, compared with the model predictions of the 2016 nesting HSI, right.

4.5 Habitat suitability: Interactions

Looking at the individual HSIs for each life stage of both SP and AFC allows a comparison of the overlap in their habitat niche. Whilst there is broad similarity in suitable habitat for each species when looking at the larger system-scale, when looking at individual riverbank areas along the length of the gorge, a difference between them does emerge in their life stage-specific requirements (Figure 25).

In general, the SP was relatively insensitive to distance a cell is from the river and hindered by periodic inundation events, though it can withstand short-term inundation and recover. On the other hand, the AFC habitat is focused on the river margin but the egg stage is highly sensitive to inundation. This makes the interaction of these two most intensely focused at this interface, and hydrologic changes through the dry season shifting this interface will shape the nature of the interaction.

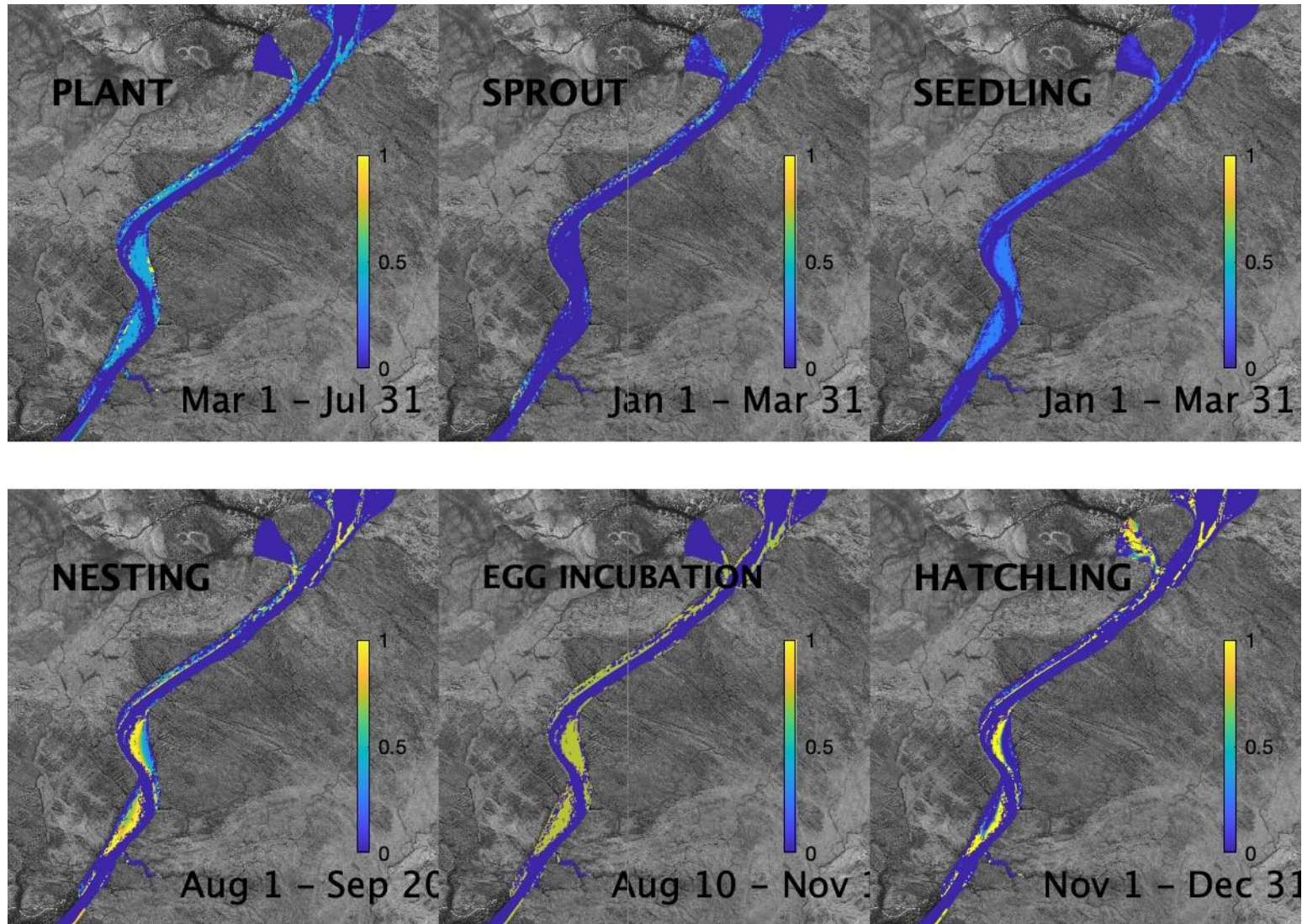


Figure 25. Summary of the habitat model output showing average HSI for different life-stages of SP and AFC within the relevant periods.

From the field monitoring surveys that were undertaken between 2016 and 2019, the co-occurrence of SP and AFC activity was commonly noted (Figure 26; Somaweera et al., 2021). The model HSI were broadly consistent with overlapping suitability along the river margins in much of the domain.

An additional analysis was undertaken to assess the extent to which AFC life-stage suitability may improve without the effect of *P. foetida* (i.e., by removing the Φ_{pss} limitation effect). The results are a map displayed by calculating the difference (Δ) of a HSI computed with and without Φ_{pss} (Figure 27). The benefit is shown to be patchy and a different pattern is seen for each life stage.

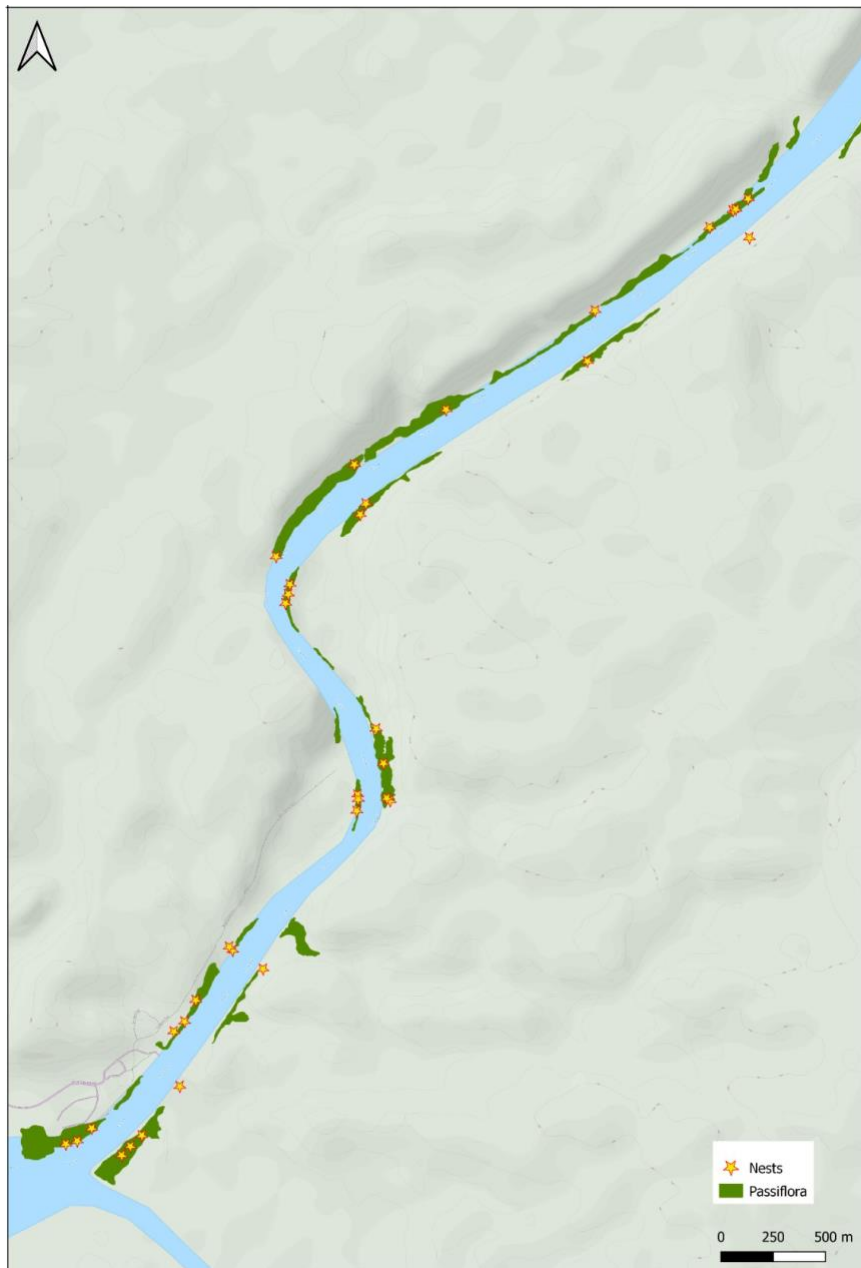


Figure 26. Monitoring data from Somaweera et al. (2021) showing identified nests and hatchling occurrence between 2016 and 2019.

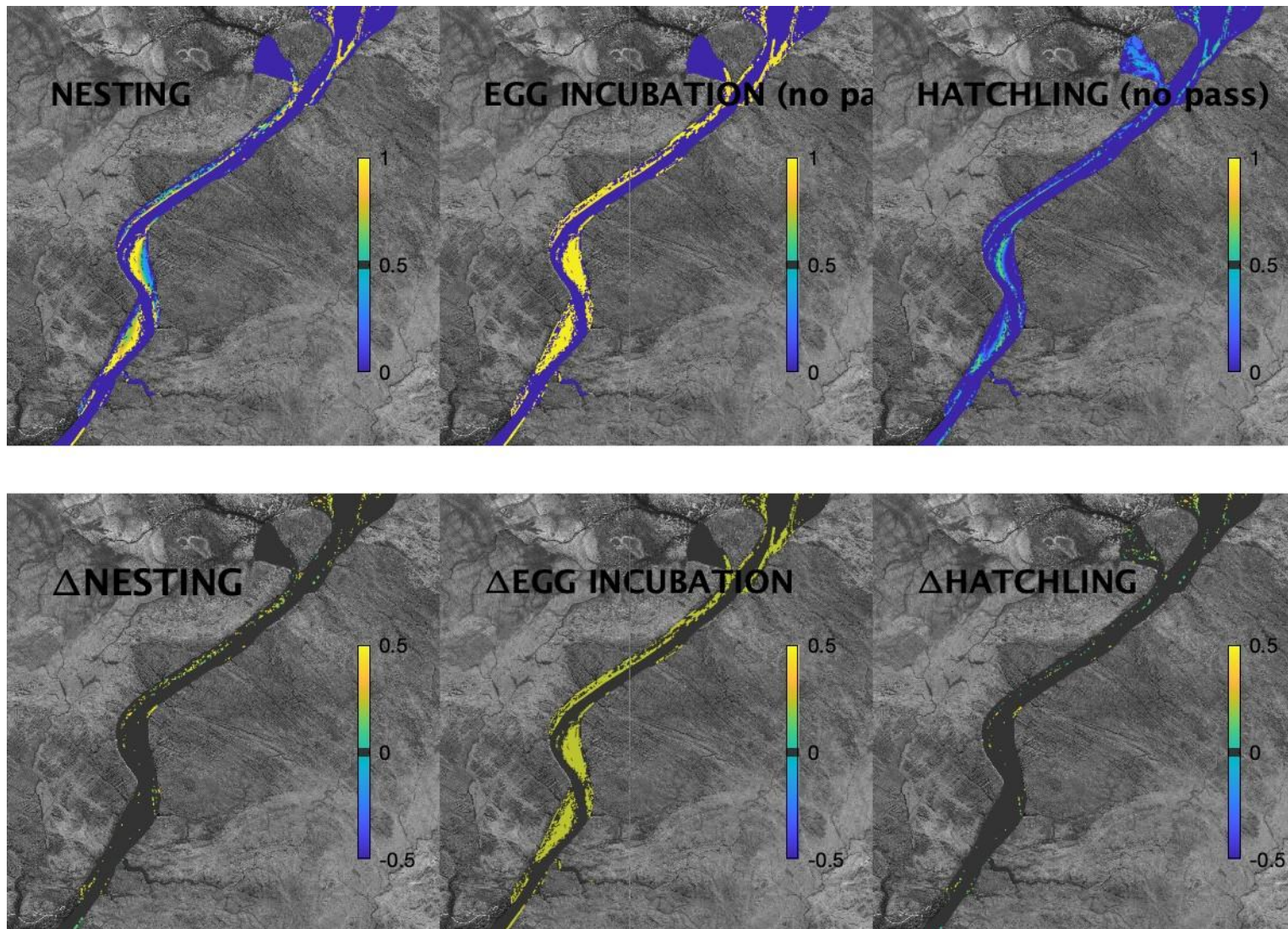


Figure 27. Summary of the habitat model output for AFC life-stages (top) and difference (Δ) if the effect of *Passiflora* is removed. Positive Δ indicates habitat expansion.

To summarise the maps, a ‘habitat quality weighted area’, over the domain is computed by summing each life-stage (Eq. 7), including for AFC with and without the SP interaction effect (Figure 28). The results show the overall niche for AFC does not expand considerably by removing the effect of *P. foetida*, though the quality of the habitat is improved.

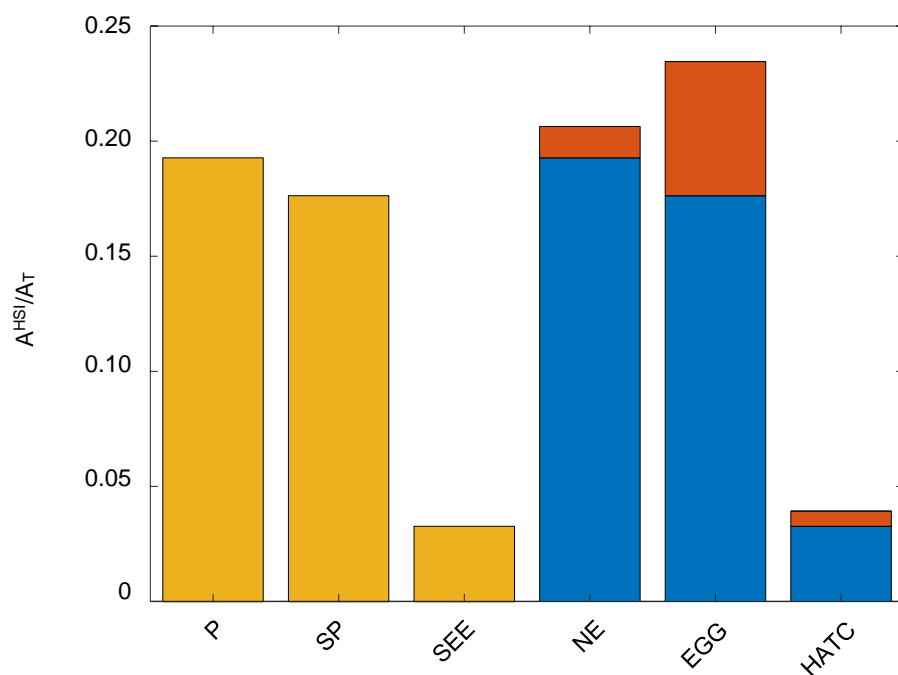
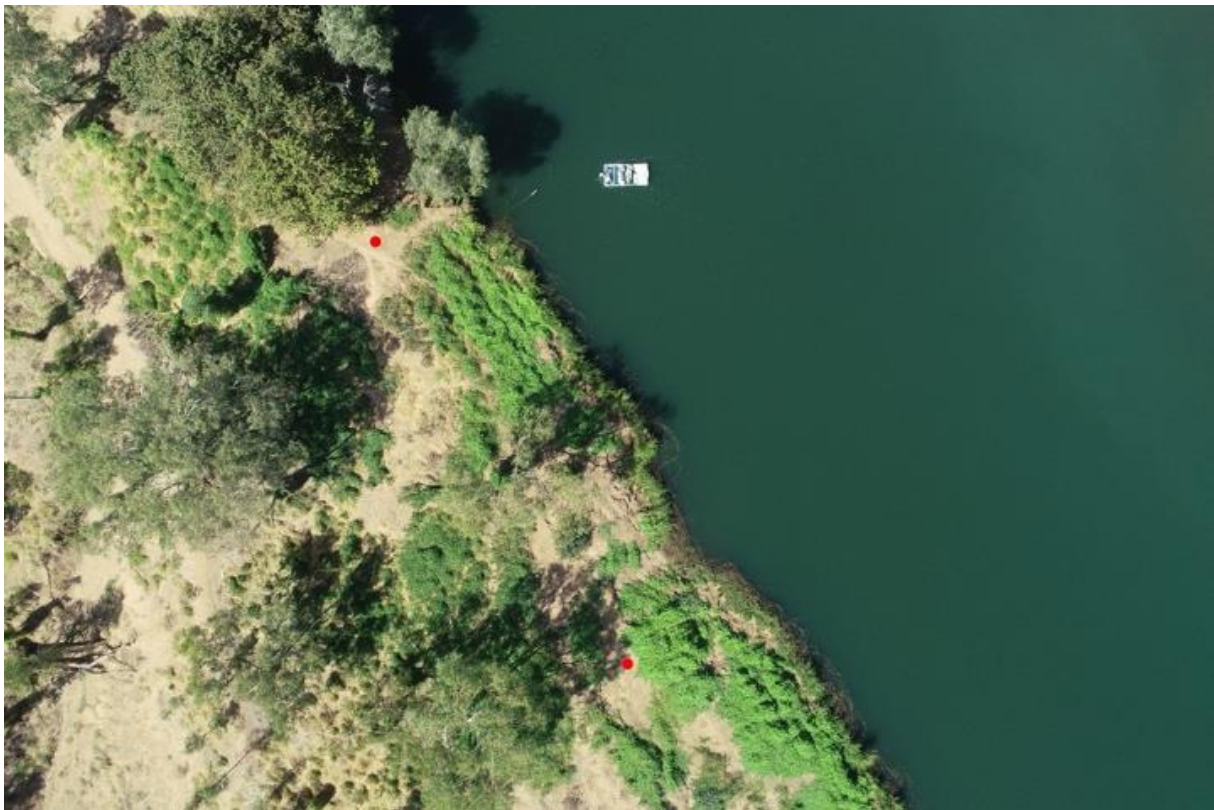


Figure 28. Effective area of suitable habitat (A^{HSI}/A_T) for different life stages of SP and AFC. The orange shaded fraction of the AFC attributes is the area that is deemed to be unsuitable due to *Passiflora* presence.

In reality, the ultimate success or failure of nesting and hatching may depend on fine-scale availability access paths and open patches (Figure 29; Somaweera et al., 2021). The model analysis here, whilst using a relatively fine mesh from a hydrologic point of view, is not able to resolve the sub-grid scale patches and paths at this scale. It may be that ultimately there is adequate habitat for nesting even in cells that are deemed poorly suitable or unsuitable based on the model analysis. The results should therefore be considered indicative of what constitutes good habitat at the macro-scale, and further effort is required to apply the model at smaller reach scales with higher resolutions. Targeted mesh creation around priority assets could also be considered.



*Figure 29. Nests (red dots) located within a *P. foetida* patch at Danggu. Note the availability of open-access paths from the water's edge to the open patch. Photo: Ruchira Somaweera.*

5. Conclusions and recommendations

To improve the management of rivers in northern Australia, tools are required that can assess impacts of changes to river water flows and support decisions associated with river and riparian zone management actions (Douglas et al. 2019). Here we have developed an integrated modelling framework, unique in its ability to resolve river dynamics and riparian zone ecohydrology. We have adapted the framework to be able to predict habitat suitability for two different but interacting species.

The present report outlines the model development and its application to the focus study site – Danggu (Geikie Gorge) – spanning the wet and dry season of 2016. With a relatively modest amount of input data (gauged river flows, weather, river and floodplain bathymetry) plus satellite imagery, we have been able to simulate river flow and riparian zone microclimate – including soil temperature and moisture – and estimate habitat area.

Whilst some broad similarity in suitable habitat for each species could be described when looking at the larger system scale, when looking at individual riverbank areas along the length of the gorge, a difference between them in their life-stage specific requirements emerges. In general, SP was relatively insensitive to the distance a cell was from the river but was hindered by periodic inundation events. On the other hand, the AFC habitat was focused on the river margin, even though the egg stage was highly sensitive to inundation. This makes the interaction of these two species most intensely focused at the river interface, and hydrologic changes through the dry season shifting this interface shape the nature of the interaction.

The time period presented is a largely static example of the model function, allowing us to develop, test and document the approach and demonstrate its utility. Next steps include application of the model to a wider range of flow conditions, both the antecedent river flow dynamics in the wet (e.g., low, medium and high flow conditions), and alternate flow realisations that may be typical of the dry season (capturing years with prolonged interflow periods, or sporadic pulse punctuating a series of shorter droughts, for example).

In addition to expanding the diversity of conditions the model is used to assess, upon reflection of the model results presented in Section 4.5, it is also a possibility to further refine the model mesh to better resolve the habitat features that may be relevant to the ecosystem. For example, the current mesh was built with the view to efficiently capture the floodplain flow pulses but redesigning the mesh to resolve the riparian margin and wetland complexity in the floodplain could greatly benefit the resolution of outputs gained from the habitat model. A newly released GPU optimised version of `TUFLOW-FV - AED` also offers 5-9x speed increases allowing for considerable refinement in the mesh resolution and longer simulation periods. Recent QGIS integration of the model platform can also assist in simplifying the model setup and analysis, allowing future survey data to be more easily incorporated and overlain with the model results.

Further development of the model to resolve lateral groundwater inputs and improved vegetation water use would help to improve its reliability in resolving the riparian zone water table and vadose zone soil moisture predictions. In this report, the model has been shown to

perform based on a limited accuracy assessment but further targeted data collection could greatly assist efforts to constrain the parameters used in the modelling.

Beyond additional environmental monitoring, efforts to develop datasets that can be used for habitat quality validation can also allow refinement of the assumptions and parameters used in this assessment. For example, temperature, velocity and soil moisture thresholds assumed in Table 3 and Table 4 can be improved over time as more targeted observations are made. Use of drones for aerial imagery or analysis with high-resolution satellite products for a wide range of hydrological conditions can assist in creating workflows for HSI validation. In this study, we made a relatively qualitative assessment of the HSI values and the results are promising, but a more robust assessment is required to transition the model approach into a practical management tool that can be used in conjunction with ongoing field surveys.

The model approach has significant potential to be used to assess scenarios linked to management of *P. foetida* spread, and also scenarios associated with flow changes brought about by water allocation in the catchment and climate change. Drought and over-allocation of water resources in southern Australia has focused attention on the potential for expanding irrigated agriculture in the north. As such, there is a renewed interest in developing and harvesting the water resources of northern Australia (Douglas et al. 2019; Pusey and Kath, 2015). Moise et al. (2015) has also suggested that northern Australia is likely to experience higher temperatures, more-frequent hot days, more-intense rainfall and more-intense cyclonic events between 2030 and 2070. Those climatic changes are likely to vary across the region and impacts may be highly localised. Inland areas may experience more extreme high temperatures, drought, flooding, dust storms and bushfires (CSIRO, 2009). These potential hydrological impacts caused by changing climate and development are not without potential risks to biodiversity and cultural values (Canham et al. 2021; Douglas et al. 2011; Green et al. 2006; Pusey and Kath, 2015). That is expected to be the case for AFC nesting sites and for *Passiflora foetida* invasion. Further application of the model to undertake a thorough assessment of the consequences of changing water availability both by natural and man-made means on both species can provide insights to help managers anticipate risks and prepare potential adaptation strategies.

Finally, we highlight that despite the specific and local nature of this investigation, the underlying tool developed here is well-supported and available for use within a wider range of application contexts. For example, the model framework has recently been applied to inland waterholes in Queensland for prediction of fish-kill risk during drought, by developing a similar HSI approach linking water depth, temperature and oxygen. The approach is attractive in that it can utilise core hydrologic and weather monitoring with river bathymetry and satellite imagery to develop deep insights into the spatiotemporal controls on species. As we increasingly subject our rivers to conditions outside those under which the communities have established, this approach provides a mechanistic alternative to predict management outcomes that empirical SDM approaches are less well-suited to.

References

- Allen, R.G., Pereira, L.S., Raes, D., and Smith, M., 1998. Crop evapotranspiration - Guidelines for computing crop water requirements, Food and Agriculture Organization of the United Nations, Rome, Italy.
- Aydin, M., Yang, S.L., Kurt, N., and Yano, T., 2005. Test of a simple model for estimating evaporation from bare soils in different environments. *Ecological Modelling*, 182(1): 91-105.
- Bolton, M., 1989. FAO Conservation Guide 22 - Collection and incubation of eggs, Food and Agriculture Organization of the United Nations, Rome, <http://www.fao.org/docrep/006/T0226E/t0226e06.htm>.
- Canham, C.A., Beesley, L.S., Gwinn, D.C., Douglas, M.M., Setterfield, S.A., Freestone, F.L., Clohessy, S. and Loomes, R.C. 2021. Predicting the occurrence of riparian woody species to inform environmental water policies in an Australian tropical river. *Freshwater Biology*.
- Chandrasena, N. R. and Johnson, S. B., 2015. Weed Management in Australia: An Overview and Prognosis. In V. S. Rao, N. T. Yaduraju, N. R. Chandrasena, Gul Hassan, A. R. Sharma (Ed.), *Weed Science in the Asian-Pacific Region*. Asian-Pacific Weed Science Society and Indian Weed Science Society.
- CSIRO, 1996. General Report on Lands of the West Kimberley Area, W.A. <http://www.publish.csiro.au/CR/pdf/LRS09>
- CSIRO, 2009. Water in northern Australia. Summary of reports to the Australian Government from the CSIRO Northern Australia Sustainable Yields Project, Australia.
- Douglas, M.M., Jackson, S., Canham, C.A., Laborde, S., Beesley, L., Kennard, M.J., Pusey, B.J., Loomes, R. and Setterfield, S.A. 2019. Conceptualizing hydro-socio-ecological relationships to enable more integrated and inclusive water allocation planning. *One Earth* 1(3), 361-373.
- Douglas, M., Jackson, S., Setterfield, S., Pusey, B., Davies, P., Kennard, M., Burrows, D., and Bunn, S. (2011). Northern futures: Threats and opportunities for freshwater systems. In Pusey, B. (ed.), *Aquatic Biodiversity in Northern Australia: Patterns, Threats and Future*. Charles Darwin University Press, Darwin, pp. 203–220
- Elith, J., and Leathwick, J.R., 2009. Species Distribution Models: Ecological explanation and prediction across space and time. *Annual Review of Ecology, Evolution, and Systematics*, 40(1): 677-697.
- Findlay, S.E., 2019. Characterising the climatic regeneration niche of stinking passionflower (*Passiflora foetida*). [Unpublished master's thesis]. The University of Western Australia.
- Gallant, J., Wilson, N., Dowling, T., Read, A. and Inskeep, C. 2011. SRTM-derived 1 Second Digital Elevation Models Version 1.0. Record 1. Geoscience Australia, Canberra.
- Green, D., 2006. Climate Change and Health: Impacts on Remote Indigenous Communities in Northern Australia, CSIRO Marine and Atmospheric Research.

- Govêa, K. P., Neto, A. R. C., Resck, N. M., Moreira, L. L., Júnior, V. V., Pereira, F. L., and Souza, T. C., 2018. Morpho-anatomical and physiological aspects of *Passiflora edulis* Sims (passion fruit) subjected to flooded conditions during early developmental stages. *Biotemas*, 31(3), 15-23.
- Hipsey, M.R., Boon, C., Paraska, D., Bruce, L.C. and Huang, P., 2019. AquaticEcoDynamics/libaed2: v1.3.0-rc2, Aquatic EcoDynamics (AED) Model Library & Science Manual, 1–34, doi:10.5281/zenodo.2538495.
- Kearney, M.R. and Porter, W.P., 2017. NicheMapR – an R package for biophysical modelling: the microclimate model. *Ecography*, 40: 664-674.
- Lang, J.W. and Andrews, H.V. 1994. Temperature dependent sex determination in Crocodilians. *Journal of Experimental Zoology*, 270(1): 28-44., 19(4): 301-306.
- Jucker, T., Long, V., Pozzari, D., Pedersen, D., Fitzpatrick, B., Yeoh, P.B. and Webber, B.L., 2020. Developing effective management solutions for controlling stinking passionflower (*Passiflora foetida*) and promoting the recovery of native biodiversity in Northern Australia. *Biological Invasions*, 22(9), pp.2737-2748.
- Magnusson W. E., 1982. Mortality of Eggs of the Crocodile *Crocodylus porosus* in Northern Australia. *Journal of Herpetology*, 16(2): 121-130.
- Mazzotti F. J., 1989. Factors affecting the nesting success of the American crocodile, *Crocodylus acutus*, in Florida Bay. *Bull. Mar. Sci.* 44, 220– 8.
- Moise, A. et al., 2015. Monsoonal North Cluster Report, CSIRO and Bureau of Meteorology, Australia.
- Pusey, B.J., Kath, J., 2015. Environmental Water Management in the Fitzroy River Valley Information availability, knowledge gaps and research needs, Perth, Western Australia.
- Skaggs, T.H., van Genuchten, M.T., Shouse, P.J., Poss, J.A., 2006. Macroscopic approaches to root water uptake as a function of water and salinity stress. *Agricultural Water Management*, 86(1-2): 140-149.
- Smith A. M. A., 1987. The sex and survivorship of embryos and hatchlings of the Australian freshwater crocodiles, *Crocodylus johnstoni* (PhD thesis). Australian National University, Canberra.
- Somaweera, R., & Shine, R., 2013. Nest-site selection by crocodiles at a rocky site in the Australian tropics: Making the best of a bad lot. *Austral Ecology*, 38, 313-325.
- Somaweera R, Greatwich B, Yeoh PB & Webber BL. 2020. Distribution maps of freshwater crocodiles and their nests at Danggu (Geikie Gorge) National Park. CSIRO, Perth
- Somaweera, R., Yeoh, P.B. and Webber, B.L. (2021) Guiding stinking passionflower management at Danggu (Geikie Gorge) National Park for conservation of freshwater crocodiles. CSIRO, Perth
- Webb G. J. W., Buckworth R. and Manolis C. S., 1983. *Crocodylus johnstoni* in the McKinlay River, N.T. VI. Nesting Biology. *Australian Wildlife Research* 10, 607– 37.

- Webb G. J. W., Manolis S. C., Whitehead P. J. & Dempsey K., 1987. The possible relationship between embryo orientation, opaque banding and the dehydration of albumen of crocodile eggs. *Copeia* 1987, 252– 7.
- Webber, B.L., Yeoh, P. B. and Scott, J.K., 2014. Invasive *Passiflora foetida* in the Kimberley and Pilbara: understanding the threat and exploring solutions. Phase 1 final report. CSIRO, Australia.
- Webber, B. L., Yeoh, P. B. and Somaweera R., 2018. Climatic limits, spatio-temporal range, and reproductive output of stinking passionflower (*Passiflora foetida*) – interim report. CSIRO, Perth
- White, K.A. 2017. Limitations to invasion success: identifying the climatic requirements of *Passiflora foetida* during germination and early establishment life phases. [Unpublished honours thesis]. The University of Western Australia.
- Ziska, L.H., Dukes, J.S., 2014. Invasive Species and Global Climate Change. CABI.

